REFERENCES

1. Heslin MJ, Lewis JJ, Nadler E, *et al.* Prognostic factors associated with long-term survival for retroperitoneal sarcoma: Implications for management. *J Clin Oncol* 1997;15:2832–2839.
2. Catton CN, O'Sullivan B, Kotwall C, *et al.* Outcome and prognosis in retroperitoneal soft tissue sarcoma. *Int J Radiat Oncol Biol Phys* 1994;29:1005–1010.
3. Ballo MT, Zagars GK, Pollock RE, *et al.* Retroperitoneal soft tissue sarcoma: An analysis of radiation and surgical treatment. *Int J Radiat Oncol Biol Phys* 2007;67:158–163.
4. Lewis JJ, Leung D, Woodruff JM, *et al.* Retroperitoneal soft-tissue sarcoma: Analysis of 500 patients treated and followed at a single institution. *Ann Surg* 1998;228:355–365.
5. Potter DA, Kinsella T, Glatstein E, *et al.* High-grade soft tissue sarcomas of the extremities. *Cancer* 1986;58:190–205.
6. Pisters PW, Harrison LB, Leung DH, *et al.* Long-term results of a prospective randomized trial of adjuvant brachytherapy in soft tissue sarcoma. *J Clin Oncol* 1996;14:859–868.
7. Yang JC, Chang AE, Baker AR, *et al.* Randomized prospective study of the benefit of adjuvant radiation therapy in the treatment of soft tissue sarcomas of the extremity. *J Clin Oncol* 1998;16:197–203.
8. Pisters PW, O'Sullivan B, Maki RG. Evidence-based recommendations for local therapy for soft tissue sarcomas. *J Clin Oncol* 2007;25:1003–1008.
9. Pisters PW, Patel SR, Prieto VG, *et al.* Phase I trial of preoperative doxorubicin-based concurrent chemoradiation and surgical resection for localized extremity and body wall soft tissue sarcomas. *J Clin Oncol* 2004;22:3375–3380.
10. Kamada T, Tsujii H, Tsuji H, *et al.* Efficacy and safety of carbon ion radiotherapy in bone and soft tissue sarcomas. *J Clin Oncol* 2002;20:4466–4471.
11. Imai R, Kamada T, Tsuji H, *et al.* Carbon ion radiotherapy for unresectable sacral chordomas. *Clin Cancer Res* 2004;10: 5741–5746.
12. Kanai T, Endo M, Minohara S, *et al.* Biophysical characteristics of HIMAC clinical irradiation system for heavy-ion radiation therapy. *Int J Radiat Oncol Biol Phys* 1999;44:201–210.
13. Cox JD, Stetz J, Pajak TF. Toxicity criteria of the Radiation Therapy Oncology Group (RTOG) and the European Organization for Research Treatment of Cancer (EORTC). *Int J Radiat Oncol Biol Phys* 1995;31:1341–1346.
14. Stoeckle E, Coindre JM, Bonvalot S, *et al.* Prognostic factors in retroperitoneal sarcoma: A multivariate analysis of a series of 165 patients of the French Cancer Center Federation Sarcoma Group. *Cancer* 2001;9:359–368.
15. van Dalen T, Hoekstra HJ, van Geel AN, *et al.* Locoregional recurrence of retroperitoneal soft tissue sarcoma: Second chance of cure for selected patients. *Eur J Surg Oncol* 2001;27:564–568.
16. Gronchi A, Casali PG, Fiore M, *et al.* Retroperitoneal soft tissue sarcomas: Patterns of recurrence in 167 patients treated at a single institution. *Cancer* 2004;100:2448–2455.
17. Gilbeau L, Kantor G, Stoeckle E, *et al.* Surgical resection and radiotherapy for primary retroperitoneal soft tissue sarcoma. *Radiother Oncol* 2002;65:137–143.
18. Krempien R, Roeder F, Oertel S, *et al.* Intraoperative electron-beam therapy for primary and recurrent retroperitoneal soft-tissue sarcoma. *Int J Radiat Oncol Biol Phys* 2006;65:773–779.
19. Youssef E, Fontanesi J, Mott M, *et al.* Long-term outcome of combined modality therapy in retroperitoneal and deep-trunk soft-tissue sarcoma: Analysis of prognostic factors. *Int J Radiat Oncol Biol Phys* 2002;54. 514–5219.
20. Fein DA, Corn BW, Lanciano RM, *et al.* Management of retroperitoneal sarcomas: Does dose escalation impact on locoregional control? *Int J Radiat Oncol Biol Phys* 1995;31:129–134.
21. Jones JJ, Catton CN, O'Sullivan B, *et al.* Initial results of a trial of preoperative external-beam radiation therapy and postoperative brachytherapy for retroperitoneal sarcoma. *Ann Surg Oncol* 2002;9:346–354.
22. Petersen IA, Haddock MG, Donohue JH, *et al.* Use of intraoperative electron beam radiotherapy in the management of retroperitoneal soft tissue sarcomas. *Int J Radiat Oncol Biol Phys* 2002; 52:469–475.
23. Tzeng CW, Fiveash JB, Popple RA, *et al.* Preoperative radiation therapy with selective dose escalation to the margin at risk for retroperitoneal sarcoma. *Cancer* 2006;107:371–379.
24. Feng M, Murphy J, Griffith KA, *et al.* Long-term outcomes after radiotherapy for retroperitoneal and deep truncal sarcoma. *Int J Radiat Oncol Biol Phys* 2007;69:103–110.
25. Guadagnolo BA, Zagars GK, Ballo MT, *et al.* Excellent local control rates and distinctive patterns of failure in myxoid liposarcoma treated with conservation surgery and radiotherapy. *Int J Radiat Oncol Biol Phys* 2008;70:760–765.

Int. J. Radiation Oncology Biol. Phys., Vol. ■, No. ■, pp. 1–7, 2009

0360-3016/09/$–see front matter

ELSEVIER

doi:10.1016/j.ijrobp.2009.06.048

CLINICAL INVESTIGATION

EFFECT OF CARBON ION RADIOTHERAPY FOR SACRAL CHORDOMA: RESULTS OF PHASE I-II AND PHASE II CLINICAL TRIALS

REIKO IMAI, M.D., PH.D.,* TADASHI KAMADA, M.D., PH.D.,* HIROSHI TSUJI, M.D., PH.D.,* SHINJI SUGAWARA, M.D., PH.D.,* ITSUKO SERIZAWA, M.D.,* HIROHIKO TSUJII, M.D., PH.D.,* AND SHINICHIRO TATEZAKI, M.D., PH.D., † FOR THE WORKING GROUP FOR BONE AND SOFT TISSUE SARCOMAS

*Research Center Hospital for Charged Particle Therapy, National Institute of Radiological Sciences, Chiba, Japan; and †Division of Orthopedic Surgery, Chiba Cancer Center, Chiba, Japan

Purpose: To summarize the results of treatment for sacral chordoma in Phase I-II and Phase II carbon ion radiotherapy trials for bone and soft-tissue sarcomas.

Patients and Methods: We performed a retrospective analysis of 38 patients with medically unresectable sacral chordomas treated with the Heavy Ion Medical Accelerator in Chiba, Japan between 1996 and 2003. Of the 38 patients, 30 had not received previous treatment and 8 had locally recurrent tumor after previous resection. The applied carbon ion dose was 52.8–73.6 Gray equivalents (median, 70.4) in a total of 16 fixed fractions within 4 weeks.

Results: The median patient age was 66 years. The cranial tumor extension was S2 or greater in 31 patients. The median clinical target volume was 523 cm^3. The median follow-up period was 80 months. The 5-year overall survival rate was 86%, and the 5-year local control rate was 89%. After treatment, 27 of 30 patients with primary tumor remained ambulatory with or without supportive devices. Two patients experienced severe skin or soft-tissue complications requiring skin grafts.

Conclusion: Carbon ion radiotherapy appears effective and safe in the treatment of patients with sacral chordoma and offers a promising alternative to surgery. © **2009 Elsevier Inc.**

Carbon ion radiotherapy, charged particle therapy, clinical trials, chordoma, bone sarcoma.

INTRODUCTION

Sacral chordomas constitute >50% of all chordomas and account for only 1–4% of all primary malignant bone tumors (1, 2). Chordomas, which arise from notochordal remnants, have slower local growth and metastasize less frequently than other bone and soft-tissue malignant tumors (1–3). They are not easy to control because of their anatomic location and propensity for spreading extensively. Although complete radical resection produces longer continuous local control and an extended disease-free period compared with subtotal resection (4–8), by the time the symptoms first appear, chordomas are often already too large for complete excision to be possible (9, 10). Thus, despite being a low-grade malignancy, sacral chordomas have a low long-term local control rate (6, 7). Sacral chordomas also have poor sensitivity to chemotherapy (1, 2). Some studies have reported that photon radiotherapy might delay recurrence after incomplete resection and might also be able to relieve the symptoms caused by recurrence (4, 7, 9).

Carbon ion beams share certain unique physical properties with proton beams. In particular, after penetrating into the body, they emit only a low radiation dose along their travel path. They then deliver their maximal dose at the end of their range, beyond which the radiation dose decreases sharply (Bragg peak). This pattern of irradiation facilitates the delivery of an optimal radiation dose to the tumor while exposing critical organs surrounding the tumor to lower doses. In contrast, hand photon beams, including X-ray beams, apply their maximal dose near the surface of the body, and the dose decreases with an increasing depth into the body. Carbon ion radiotherapy (CIRT) can thus provide a superior dose distribution to nonsurface tumors compared with photon radiotherapy.

A distinctive property of carbon ion beams distinguishing them from proton beams is their high biologic effectiveness. Carbon ion beams deliver a larger mean energy per unit length of their trajectory (*i.e.*, greater linear energy transfer [LET]) to the body tissues than photon and proton beams.

Reprint requests to: Reiko Imai, M.D., Ph.D., Research Center Hospital for Charged Particle Therapy, National Institute of Radiological Sciences, Anagawa 4-9-1, Inage-ku, Chiba 263-8555 Japan. Tel: (+81) 43-251-2111; Fax: (+81) 43-206-6506; E-mail: r_imai@nirs.go.jp

Supported by the Research Project with Heavy Ions at National Institute of Radiological Sciences–Heavy Ion Medical Accelerator in Chiba of the National Institute of Radiological Sciences.

Conflict of interest: none.

Received March 3, 2009, and in revised form June 22, 2009. Accepted for publication June 22, 2009.

Furthermore, the LET of carbon ion beams increases steadily from the initial value at the entrance point as it passes through the body, reaching its maximal value at the end of its range. These advantageous treatment profiles for carbon ion beams are likely responsible for the good results with treatment of sacral chordoma, as previously reported (10).

Since 1996, we have been involved in clinical trials of CIRT for medically inoperable bone and soft-tissue sarcomas at the National Institute of Radiological Sciences, Chiba, Japan. The first Phase I-II dose-searching clinical trial was implemented between June 1996 and February 2000, followed by a Phase II fixed-dose clinical trial between April 2000 and October 2003 (11). After these trials, CIRT was approved as advanced medical technology for heavy particle radiotherapy by the Ministry of Health in Japan in October 2003.

PATIENTS AND METHODS

Patients

The patients meeting all the following eligibility criteria were registered for the Phase I-II and Phase II CIRT trials for bone and soft-tissue sarcomas: tumor deemed to be medically inoperable by the referring surgeons; no distant metastasis at the initial referral for treatment; no previous radiotherapy at the same site; a Karnofsky performance status score of >60; and a grossly measurable tumor.

All patients signed an informed consent form approved by the local institutional review board. The details of eligibility for these trials have been previously published (10–12).

Carbon ion radiotherapy

The specific technique of CIRT used at the National Institute of Radiological Sciences has been previously described in detail (10–16). The heavy ion medical accelerator in Chiba generates carbon ion beams with accelerated energies of 290 MeV/n, 350MeV/n, and 400 MeV/n. These energy beams have a range of 15–25 cm water equivalent depth. For modulation of the Bragg peak to conform to a target volume, the beam lines for treatment are equipped with a pair of wobbler magnets, beam scatterers, ridge filters, multileaf collimators, and compensation bolus. The ridge filter is designed to produce biologically equal effects along the spread-out Bragg peak. The energies of 350 and 400 MeV/n are used mainly for treatment of sacral chordomas.

The patients were positioned in customized cradles and immobilized with a low-temperature thermoplastic sheet. A series of computed tomography (CT) images with a 5-mm slice thickness was taken for treatment planning. Respiratory gating for both CT acquisition and therapy was performed when indicated (13, 14). We began applying respiratory gating because we had observed moving skin lines on the planning CT images.

Three-dimensional treatment planning of CIRT was performed using the HIPLAN software program (National Institute of Radiological Sciences, Chiba, Japan) (15, 16). The planning target volume (PTV) included the clinical target volume plus a 5-mm safety margin for positioning errors. The tumor extent was evaluated by magnetic resonance imaging, CT, and positron emission tomography. In cases in which the tumor was located close to critical organs, such as the bowel, the margin was reduced accordingly.

The clinical target volume was covered by ≥90% of the prescribed dose (Fig. 1). We used dosages of 52.8–73.6 Gray equivalents (GyE) (carbon physical dose in Gray × relative biologic effectiveness [RBE]) on the basis of the results from previous trials of bone and soft-tissue tumors (10, 11). The RBE was evaluated using both radiobiologic and physical studies (15, 16). CIRT was performed once daily, 4 d/wk (Tuesday to Friday), for a total of 16 fixed fractions within 4 weeks. Two to four irregularly shaped ports were applied. One port was treated in each session. At every treatment session, patient positioning was confirmed with a computer-aided, on-line positioning system. The median clinical target volume of the tumors was 523 cm^3 (range 135–1,468). Of the 38 patients, 1 received a total dose of 54.8 GyE, 1 a dose of 64.0 GyE, 29 a dose of 70.4 GyE, and 7 received a total dose of 73.6 GyE. One huge tumor was divided into two fields because it was spreading into the right and left gluteus muscles.

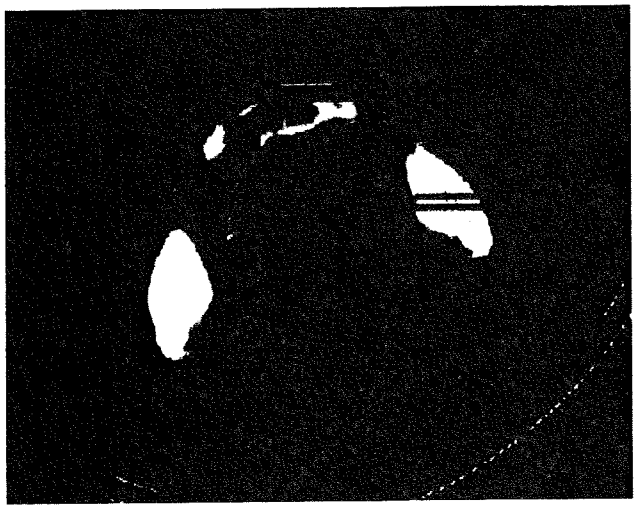

Fig. 1. Dose distribution of carbon ion beams in sacral chordoma. Red line represents 90% isodose of prescribed dose 70.4 GyE using three ports.

Statistical analysis

The patients were closely monitored through physical examinations, CT, and magnetic resonance imaging. The initial follow-up examinations were performed at the end of CIRT and again 1–2 months after CIRT completion. We planned subsequent follow-up visits to check the progress of our patients at our hospital at least every 6 months. However, for some patients, who were elderly or lived in remote places, our only recourse was to estimate their condition using imaging films taken at local hospitals and the medical reports from their local doctors.

The follow-up period was calculated from the initial date of CIRT. Recurrence was defined as tumor regrowth (*i.e.*, an increase in tumor volume observed on two consecutive magnetic resonance imaging or CT scans). The mode of failure in the present study was defined as follows: local failure, relapse within the PTV; marginal failure, relapse within 2 cm of the PTV; and distant failure, tumor growth identified >2 cm from the PTV.

The local control and overall survival rates were calculated using the Kaplan-Meier method. The log–rank test was used for individual comparisons. The last follow-up date was August 2008, with the exception of 1 patient who had not been located for 34 months after treatment.

RESULTS

Between June 1996 and October 2003, 39 patients with sacral chordoma were registered for the trials. After registration, 1 patient was excluded from analysis because only

cytologic specimens were available, leaving 38 evaluable patients with sacral chordoma treated with CIRT. All tumors were pathologically confirmed as chordomas by the pathologist at the referral hospital and our pathologists.

The study patients included 29 men and 9 women. Their median age was 66 years (range 41–85). The median Karnofsky performance status score was 80 (range 70–90). Of the 38 patients, 30 had received no previous treatment, and 8 had tumor recurrence after previous surgical resection. The initial surgical treatment of these 8 patients had included intralesional resection in 2 patients, marginal resection in 3, and unknown resection type in 3. All tumors had originated in the sacrum. The characteristics of the 38 study patients are summarized in Table 1.

Tumor response and survival for all patients

All 38 patients completed CIRT. The median follow-up period was 80 months, and median survival time was 70 months (range, 13–122). The 3- and 5-year local control rate was 95% and 89%, respectively (Figs. 2 and 3). Four patients developed local treatment failure that occurred inside the irradiation field at 13, 35, 48, and 59 months after CIRT. The failure at 13 months occurred in the patient whose tumor had had the largest volume (1,468 cm^3). The failure at 48 months occurred in 1 patient from the previous surgery group. The patients with the local failure at 59 months and 48 months underwent salvage CIRT. Additional tumor growth was controlled through the last follow-up visit.

The 3- and 5-year overall survival rate was 95% and 86%, respectively (Fig. 4). The 3-and 5-year progression-free survival rates was 76% and 54%, respectively (Fig. 5). During the entire observation period, 12 patients died. Of these 12 patients, 5 died of their tumor. Of the remaining 7 patients, 4 died of intercurrent disease, such as brain hemorrhage or infection, without local or systemic recurrence. The direct causes of death for the other 3 patients was intercurrent disease such as senility, urinary tract infection, and another cancer with distant metastases. One patient had a lumbar spine metastasis treated with CIRT 29 months after the CIRT, and it was controlled until death 8.5 years later. Another patient with distant metastasis in the femoral muscle that was controlled with CIRT died of gastric cancer. The third patient had pelvic metastasis controlled by CIRT and died of a urinary tract infection 26 months after treatment.

Distant metastases occurred in 15 patients. The most frequent sites were the lung (6 patients) and bone (5 patients). Of these 15 patients, the median time from the first day of CIRT to the diagnosis of distant metastases was 40 months (range, 1–62); 9 patients underwent salvage treatment with repeated CIRT. Four patients had multiple metastases; these patients were in the group of 8 patients with locally recurrent tumors after previous surgery. Additional analysis found that the patients with locally recurrent tumors after previous surgery had a significantly greater incidence of distant metastases after CIRT compared than the patients who had received no treatment before CIRT ($p = .001$).

Table 1. Patient characteristics

Characteristic	Value
Patients (*n*)	38
Gender	
Male	29
Female	9
Age (y)	
Median	66
Range	41–85
Previous surgery	
Yes	8
No	30
Most proximal tumor level	
L5	6
S1	10
S2	15
S3	4
S4	1
Intrapelvic	2
Irradiation dose (GyE/16 fractions)	
52.8	1
64.0	1
70.4	29
73.6	7

Post-RT functional evaluations

Functional evaluations after CIRT were performed for the 30 patients without previous surgery (Table 2). For the 27 patients without local recurrence, the last follow-up day was considered the date the evaluation. For the 3 patients with local recurrence, the last follow-up date was the last examination before the diagnosis of local failure. For the 30 patients, the most proximal level of tumor involvement was distributed as follows: 5 patients at L5, 10 at S1, 11 at S2, 3 at S3, and 1 patient at S4. The functional status and identification of pain medication use after CIRT are summarized in Table 2. Regarding ambulatory function, 16 patients did not require any supportive devices, and 2 patients used wheelchairs in daily life but also retained the ability to stand and walk several steps.

After CIRT, 5 patients required catheterization. All were patients who had required catheterization before CIRT; no new patients required urinary catheterization after CIRT. One patient who had required catheterization before CIRT was able to function without catheterization after CIRT. Twelve patients did not require bladder control pads after CIRT. Some of these patients had minor complaints, and others did not. Five patients who did not use control pads before CIRT experienced deterioration in their urinary function after CIRT. These 5 had had tumors extending to S1, S2, or S3 on the cranial side. Of these 5 aggravated cases, 1 was a patient who had experienced a sacral bone fracture 9 months after CIRT that was followed by occasional incontinence. A second patient developed a pelvic fracture from a traffic accident 9 months after CIRT that was followed by occasional incontinence. Of the 5 cases, 2 were recurrent. Finally, 9 patients who had complained of incontinence or who had had no sensation of urination before CIRT experienced no improvement in these symptoms

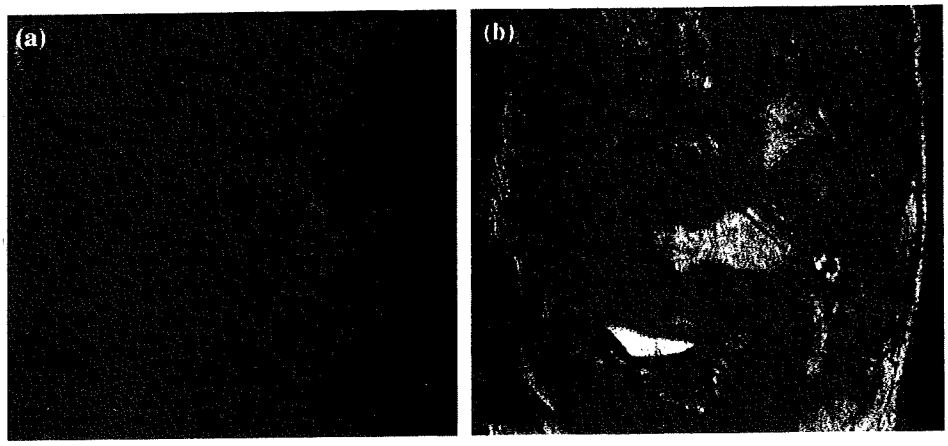

Fig. 2. Sacral chordoma revealed on T_2-weighted images. (a) Tumor before treatment. (b) Tumor had obviously shrunk at 6 years after carbon ion radiotherapy.

With respect to anorectal function, 19 patients did not require control pads after CIRT; some had minor complaints, and others did not. A total of 5 patients had undergone colostomy either before or after CIRT; 2 had undergone colostomy because of bowel obstruction before referral to our hospital. A third patient developed severe bowel obstruction during hospitalization; however, because the obstruction had resulted from the tumor compressing the rectum, the colostomy was deferred until after CIRT completion to prevent irradiation of a new colostomy. A fourth patient underwent colostomy subsequent to local recurrence after CIRT.

Of the 30 patients, 3 had had no sensation of defecation before treatment. After CIRT, 1 eventually underwent colostomy, 1 experienced transient improvement but with subsequent relapse, and 1 had no change in their condition after CIRT.

With respect to pain medication, before CIRT, 11 had been taking narcotic drugs and 1 had been receiving epidural anesthesia. At their last evaluation, 4 of the patients using narcotic drugs before CIRT were free of narcotics and 6 still used them. The patient receiving epidural anesthesia was successfully transferred to an oral narcotic drug and was able to return to part-time work.

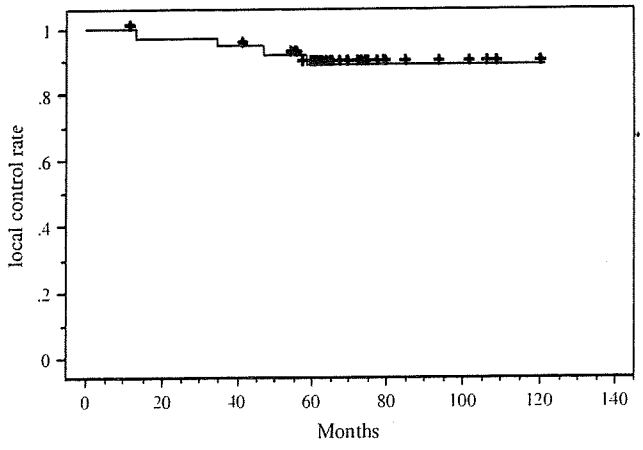

Fig. 3. Local control rate at 3 and 5 years was 95% and 89%, respectively.

With respect to general function after CIRT, 9 patients returned to work and 4 were able to continue daily activities as housewives. Four patients quit working, and one reported difficulty with housework. Twelve patients had already retired when their disease was diagnosed.

Adverse reactions

Adverse reactions to CIRT were evaluated using the National Cancer Institute Common Toxicity Criteria, version 2.0, for acute reactions. Late reactions were evaluated using the Late Effects of Normal Tissue/Subjective, Objective, Management, and Analytic scoring system, in addition to the Radiation Therapy Oncology Group/European Organization for Research and Treatment of Cancer late scoring system (17, 18).

No cases of fatal toxicity occurred during the follow-up period after CIRT. Three patients had Grade 3 acute skin reactions, two had Grade 3 late skin reactions, and two had Grade 4 late reactions that required skin grafts. No patient required a colostomy because of toxicity from CIRT. One patient developed transient Grade 1 rectal bleeding 20 months after CIRT. Of the patients with urinary dysfunction, none required urinary diversion or insertion of a permanent catheter because of bladder toxicity. As mentioned in the previous section, 1 patient had a sacral bone fracture 9 months after CIRT.

Ten patients had temporary or permanent neurologic complications. The most proximal tumor level in these 10 patients was L5 in 3, S1 in 3, S2 in 3, and S3 in 1. The radiation dosage for these 10 patients was 73.6 GyE in 4 and 70.4 GyE in 6. Of these 10 patients, 3 developed severe and permanent neurologic impairment. One had a tumor extending to the S1 level and received 73.6 GyE 95 months after CIRT. The patient still required narcotic agents and a wheelchair. Another patient, who had a tumor extending to the S1 and had received 70.4GyE, still required narcotic agents and a walker 87 months after CIRT. Neither patient had any change in symptoms related to urinary and anorectal incontinence after CIRT. The other patient with an asymptomatic S3 tumor that had been detected as an incidental finding received 70.4 GyE;

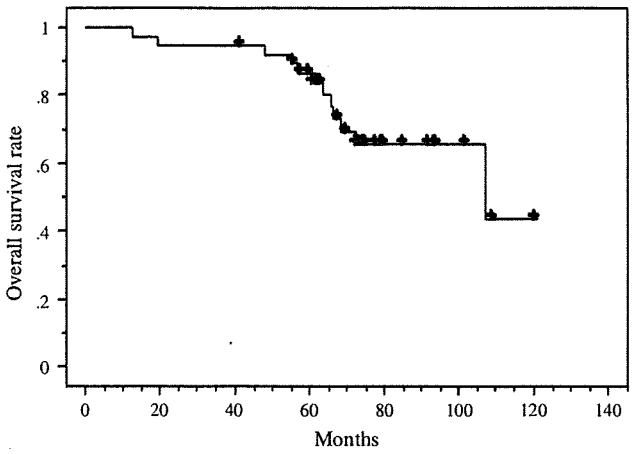

Fig. 4. Overall survival rate at 3 and 5 years was 95% and 86%, respectively.

however, the irradiated area covered the whole sacrum because small lesions had been detected that were considered to be possible "skip" lesions. This patient still required a cane, anxiolytic agents, and urinary control pads 81 months after CIRT.

DISCUSSION

Resection remains the first choice of treatment of sacral chordoma. Complete resection contributes to a good local control rate and prolongation of the disease-free survival (4–8). Local control rates have approached 60–80% for total excision cases compared with 25–50% after subtotal resection (4, 5, 7). When performing a resection, it is important not only to achieve complete resection, but also to preserve sacral nerve function. However, when a tumor extends to S2 or higher, complete resection will produce impairment of the bladder and anorectal function and a walking disability. Thus, in such cases, surgeons face the dilemma of achieving complete resection with adequate surgical margins at the expense of extirpating the patient's sacral nerves.

Furthermore, tumor seeding and contamination during surgical intervention has led to a high local recurrence rate. Kaiser *et al.* (19) reported a 64% recurrence rate after tumor spillage vs. a 28% recurrence rate without tumor spillage. However, no other treatment method such as chemotherapy or photon radiotherapy has approached the effectiveness of surgery for sacral chordomas. Several studies have shown some benefit from photon RT in a few situations (1, 4, 7, 9, 20). For instance, RT after resection effectively delays local recurrence and prolongs the disease-free interval and symptomatic relief (4, 8, 9). However, photon radiotherapy alone rarely cures cases involving visible residual tumor or unresectable tumor (9, 20).

Several reports have examined charged particle therapies for sacral chordoma. The advantage of charged particle beams is their superior dose distribution compared with photon beams. In 1993, Schoenthaler *et al.* (21), at the Lawrence Berkley Laboratory, reported a 5-year local control rate of 55% for 14 postoperative patients with sacral chordomas treated by charged neon and helium particles. They applied rather high doses (72.3–80.5 GyE) to the tumors. However, the investigators recommended maximum debulking of the tumor by radical surgery for tumor control. The Lawrence Berkley Laboratory study demonstrated a trend toward improved local control rates using neon (high LET) rather than helium (low LET).

In 2004, Schulz-Ertner *et al.* (22) reported the results of CIRT in 152 patients at the Gesellschaft für Schwerionenforschung (GSI), 8 of whom had sacral chordomas. The treatment sequence consisted of surgery, postoperative intensity-modulated RT, and a carbon ion boost to the macroscopic residual tumor. The median photon dose applied was 50.4 Gy, and the carbon ion boost was 18 GyE. One patient developed local recurrence (*i.e.*, recurrence inside the irradiated field).

DeLaney *et al.* (23) reported the results from a Phase II trial of high-dose photon/proton RT for spinal tumors at the Massachusetts General Hospital (MGH), including 29 spinal chordomas, as a part of a treatment regimen consisting of surgery plus postoperative photon and proton therapy. Before that trial, a pilot study of axial skeleton tumors treated with combined high-dose proton/photon RT suggested that the following treatment changes might improve the local control rate: primary tumor, target dose >77 Gy RBE, and total resection of the gross tumor (24). In the Phase II trial, the median applied dose was 76.6 Gy RBE. Three patients with locally recurrent sacral chordoma after previous surgery developed local failure after the treatment, but none of the patients with primary chordomas did so. The 5-year actual recurrence rate was 33% after R2 resection. In the case of biopsy, it was 13% (24).

Rutz *et al.* (25) reported the results from the Paul Scherrer Institute in Switzerland. Their treatment protocol involved either a combination of function-preserving surgery and spot-scanning proton therapy or a combination of function-preserving surgery, spot-scanning proton therapy, and photon therapy. The study included 26 patients with spinal chordomas. Of the 26 patients, 7 with sacrococcygeal chordoma and a residual tumor volume <500 cm^3 were enrolled. The median total applied dose was 72 CGE. The report did

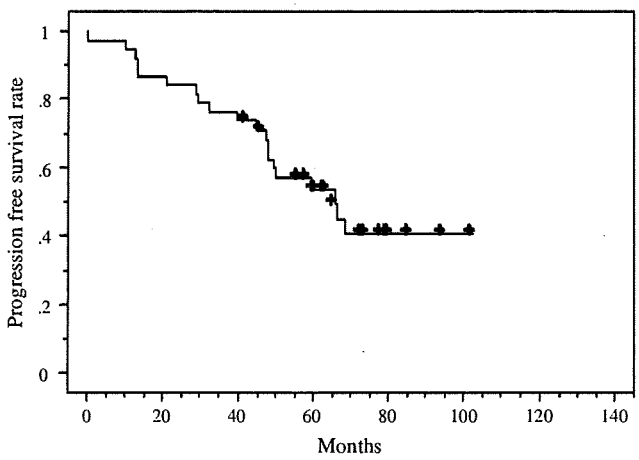

Fig. 5. Progression-free survival rate at 3 and 5 years was 76% and 54%, respectively.

Table 2. Functional evaluation results after CIRT

Finding	Patients (*n*)
Ambulatory	
Without any support devices	16
With a cane	8
With walker	3
With wheelchair	3
Total	30
Anorectal function	
Colostomy	4
Control pads	7
No pads/no complaints	19
Total	30
Urination	
Catheterization	5
Control pads	13
No pads/no complaints	12
Total	30
Pain medication	
Nonsteroidal anti-inflammatory drugs or neural agents	7
Narcotics	9
None	14
Total	30

not present location-specific results, but the 3-year local control rate for all patients was 86%. This percentage was greater than the local control rate in the MGH study (23), although the follow-up period was shorter at 35 months.

Comparing the results of these studies, the results from our study (3- and 5-year local control rate of 95% and 89%, respectively) were superior to the previously published results, assuming all our tumors were unresectable. Of the 38 tumors in our study, 21 had volumes >500 cm^3. Thus, these results indicate that CIRT for sacral chordoma represents a promising alternative to surgery and that among the various charged particle therapies available for use, the carbon ion beam has the best potential to avoid radiation-induced injuries to critical organs while administering doses sufficient for tumor control.

DeLaney *et al.* (23) reported that 2 patients with Grade 3 sacral neuropathy had received 77.4 Gy RBE and that no patients developed neural injuries at doses of ≤70.2 Gy RBE. These results are supported by the finding reported by their group that tolerance dose to the cauda equina 5 years after treatment (50% risk at 5 years) was 72 CGE for men and 84 CGE for women (26).

As we have accumulated patients with long follow-up periods, we have begun to observe cases involving aggravation of sacral nerve function after CIRT. In the 10 such cases from the presented 38 patients, 4 had received 73.6 GyE and 6 had received 70.4 GyE.

Although our experience suggests that 73.6 GyE is a dose level that could cause neurologic toxicity, we could not directly compare our experience with the studies from MGH (23, 26). The fraction dose was <2 Gy RBE at MGH. In contrast, we used a fraction dose of 4.4 GyE and 4.6 GyE, corresponding to a total dose of 70.4 GyE and 73.6 GyE, respectively. The RBE of carbon ion beams for the sacral nerve or chordoma itself has not yet been determined. However, we found that the tumor location and the irradiated area correlated with the development of neurologic impairment. Of our 10 patients with neurologic complications, all had undergone CIRT above S2. Conversely, our study included 3 patients with S3-S4 tumors without adverse reactions. Even though these patients were judged to have medically inoperable tumors by the referral surgeons, their activities of daily life after CIRT remained unchanged from those before CIRT (excellent), and none developed urinary or anorectic incontinence or an ambulatory disability. Considering this result, CIRT also has the possibility to be an alternative to surgery for resectable cases.

Patients with sacral chordomas tend to be elderly at diagnosis (1–4). The median age in our study was 66 years. The MGH group reported in 2006 that the average age of their patients with primary chordoma treated by surgery and proton beam therapy was 56 years, an average of 10 years younger than our study group (27). The study by Rutz *et al.* (25) reported an average age of 49 years, but their data set included tumors other than chordomas. Considering the effect of aging after treatment, the remnant ability of the patients shown by our data was acceptable.

The data from the present study have indicated that CIRT has efficacy against sacral chordomas and the toxicity is limited. Although more patients need to be monitored for a longer period to prove the effectiveness of CIRT, the main treatment of chordomas in the sacrum (S2 or higher) without a surgical indication might be CIRT. Even for patients with tumors low in the sacrum (S3 or S4) who are good candidates for surgery, CIRT might represent an alternative to surgery. Clinical trials are needed to compare the effectiveness and toxicity of CIRT vs. proton beam therapy.

CONCLUSION

We observed promising results from CIRT with the heavy ion medical accelerator in Chiba for unresectable sacral chordoma. We found excellent overall survival and local control rates and preservation of the sacral nerve function. Although late sacral nerve toxicity was observed in a few patients, the late adverse reactions have been acceptable to date.

REFERENCES

1. Sundaresan N. Chordomas. *Clin Orthop* 1986;204:135–142.
2. Sundaresan N, Galicich JH, Chu FC, *et al.* Spinal chordomas. *J Neurosurg* 1979;50:312–319.
3. Mindell ER. Chordoma. *J Bone Joint Surg Am* 1981;63: 501–505.
4. York JE, Kaczaraj A, Abi-Said D, *et al.* Sacral chordoma: 40-Year experience at a major cancer center. *Neurosurgery* 1999; 44:74–79.
5. Ozaki T, Hillmann A, Winkelmann W. Surgical Treatment of sacrococcygeal chordoma. *J Surg Oncol* 1997;64:274–279.

6. Yonemoto T, Tatezaki S, Takenouchi T, *et al.* The surgical management of sacrococcygeal chordoma. *Cancer* 1999;85:878–883.
7. Cheng EY, Ozerdemoglu RA, Transfeldt EE, *et al.* Lumbosacral chordoma: prognostic factors and treatment. *Spine* 1999;24: 1639–1645.
8. Bergh P, Kindblom LG, Gunterberg B, *et al.* Prognostic factors in chordoma of the sacrum and mobile spine: A study of 39 patients. *Cancer* 2000;88:2122–2134.
9. Catton C, O'Sullivan B, Bell R, *et al.* Chordoma: Long-term follow-up after radical photon irradiation. *Radiother Oncol* 1996; 41:67–72.
10. Imai R, Kamada T, Tsuji H, *et al.* Carbon ion radiotherapy for unresectable sacral chordomas. *Clin Cancer Res* 2004;10: 5741–5746.
11. Kamada T, Tsujii H, Tsuji H, *et al.* Efficacy and safety of CIRT in bone and soft tissue sarcomas. *J Clin Oncol* 2002;20: 4466–4471.
12. Tsujii H, Mizoe J, Kamada T, *et al.* Clinical results of carbon ion radiotherapy at NIRS. *J Radiat Res (Tokyo)* 2007;48(Suppl. A): A1–A13.
13. Minohara S, Kanai T, Endo M, *et al.* Respiratory gated irradiation system for heavy-ion radiotherapy. *Int J Radiat Oncol Biol Phys* 2000;47:1097–1103.
14. Kamada T, Tsujii H, Mizoe JE, *et al.* A horizontal CT system dedicated to heavy-ion beam treatment. *Radiother Oncol* 1999;50:235–237.
15. Kanai T, Endo M, Minohara S, *et al.* Biophysical characteristics of HIMAC clinical irradiation system for heavy-ion radiation therapy. *Int J Radiat Oncol Biol Phys* 1999;44:201–210.
16. Kanai T, Furusawa Y, Fukutsu K, *et al.* Irradiation of mixed beam and design of spread-out Bragg peak for heavy-ion radiotherapy. *Radiat Res* 1997;147:78–85.
17. Cox JD, Stetz J, Pajak TF. Toxicity criteria of the Radiation Therapy Oncology Group (RTOG) and the European Organization for Research and Treatment of Cancer (EORTC). *Int J Radiat Oncol Biol Phys* 1995;31:1341–1346.
18. LENT-SOMA tables. Table of contents. *Radiother Oncol* 1995; 35:17–60.
19. Kaiser TE, Pritchard DJ, Unni KK. Clinicopathologic study of sacrococcygeal chordoma. *Cancer* 1984;53:2574–2578.
20. Amendola BE, Amendola MA, Oliver E, *et al.* Chordoma: Role of radiation therapy. *Radiology* 1986;158:839–843.
21. Schoenthaler R, Castro JR, Petti PL, *et al.* Charged particle irradiation of sacral chordomas. *Int J Radiat Oncol Biol Phys* 1993;26:291–298.
22. Schulz-Ertner D, Nikoghosyan A, Thilmann C, *et al.* Results of carbon ion radiotherapy in 152 patients. *Int J Radiat Oncol Biol Phys* 2004;58:631–640.
23. DeLaney TF, Liebsch NJ, Pedlow FX, *et al.* Phase II study of high-dose photon/proton radiotherapy in the management of spine sarcomas. *Int J Radiat Oncol Biol Phys* 2009;74: 732–739.
24. Hug EB, Fitzek MM, Liebsch NJ, *et al.* Locally challenging osteo- and chondrogenic tumors of the axial skeleton: Results of combined proton and photon radiation therapy using three-dimensional treatment planning. *Int J Radiat Oncol Biol Phys* 1995;31:467–476.
25. Rutz HP, Weber DC, Sugahara S, *et al.* Extracranial chordoma: Outcome in patients treated with function-preserving surgery followed by spot-scanning proton beam irradiation. *Int J Radiat Oncol Biol Phys* 2007;67:512–520.
26. Pieters RS, Niemierko A, Fullerton BC, *et al.* Cauda equina tolerance to high-dose fractionated irradiation. *Int J Radiat Oncol Biol Phys* 2006;64:251–257.
27. Park L, DeLaney TF, Liebsch NJ, *et al.* Sacral chordomas: Impact of high-dose proton/photon-beam radiation therapy combined with or without surgery for primary versus recurrent tumor. *Int J Radiat Oncol Biol Phys* 2006;65:1514–1521.

Changes in Tumor Volume of Sacral Chordoma After Carbon Ion Radiotherapy

Itsuko Serizawa, MD, Reiko Imai, MD, PhD,* Tadashi Kamada, MD, PhD,* Hiroshi Tsuji, MD, PhD,* Riwa Kishimoto, MD, PhD,* Susumu Kandatsu, MD,* Hirohiko Tsujii, MD, PhD,* and Shin-ichiro Tatezaki, MD, PhD†*

Objective: We evaluated changes in tumor volume in cases of sacral chordoma after carbon ion radiotherapy.

Methods: Thirty-four patients with sacral chordoma underwent carbon ion radiotherapy between June 1996 and June 2003. We assessed 23 patients without previous surgery using T2-weighted magnetic resonance imaging. The tumor volume was calculated semiautomatically.

Results: Two cases showed local recurrence. The median interval of this examination was 46 months. At the end of the treatment, the tumor showed an enlargement larger than 10% of its volume in 13 of the 23 cases, no change in 4 cases, and regression in 6 cases. At the last examination, 20 cases showed a reduction in tumor volume, and the median ratio, determined as the tumor volume at the last examination divided by that before the treatment, was 0.36.

Conclusions: An increase in tumor volume at the end of the treatment does not indicate the ineffectiveness of carbon ion radiotherapy.

Key Words: chordoma, charged particle therapy, radiotherapy, magnetic resonance (MR) imaging

(*J Comput Assist Tomogr* 2009;33: 795–798)

Chordomas are rare malignant bone tumors that constitute between 1% and 4% of all primary bone malignancies.[1] About 50% of all chordomas originate in the sacrum.[1] Complete resection is the preferred method for treating chordomas for continuous local control and survival prolongation.[1] However, chordomas are often too large at the time of diagnosis for successful resection. Currently, there is no effective chemotherapy regimen for chordomas.[2–4] Because chordomas are radioresistant, photon radiotherapy is not sufficient as a curative local treatment.[2,3] As previously reported, we have treated unresectable sacral chordomas using carbon ion radiotherapy since 1996 and have achieved good results.[5] Carbon ion radiotherapy provides excellent dose distribution and high biological effectiveness. These advantages are useful for the treatment of chordomas.[5–7] In this study, we report on changes in the tumor volume of sacral chordomas after carbon ion radiotherapy. There have been no previous reports on longitudinal changes in images of chordomas that could not be surgically treated because local control could rarely be accomplished by photon radiotherapy in unresectable cases.[2–4,8] This is the first report on the longitudinal changes in images of chordoma after carbon ion radiotherapy.

From the *Research Center Hospital for Charged Particle Therapy, National Institute of Radiological Sciences, Chiba, Japan; and †Division of Orthopedic Surgery, Chiba Cancer Center, Chiba, Japan.

Received for publication June 25, 2008; accepted September 22, 2008.

Reprints: Tadashi Kamada, PhD, Research Center Hospital for Charged Particle Therapy, National Institute of Radiological Sciences, Anagawa 4-9-1, Inage-ku, Chiba 263-8555, Japan (e-mail: t_kamada@nirs.go.jp).

MATERIALS AND METHODS

Patient Characteristics

We examined 34 patients with sacral chordoma who were candidates for clinical trials and underwent carbon ion radiotherapy between June 1996 and June 2003 at the National Institute of Radiological Sciences in Chiba, Japan.[5,6] Patients eligible for phase I/II or phase II trials of carbon ion radiotherapy for bone and soft tissue sarcomas were those with tumors judged unresectable by orthopedic surgeons or those who were refused surgery. Details regarding these trials are described in a previous report.[6] Pathological specimens from each patient were reviewed, and all were confirmed as chordomas. All patients signed an informed consent form that was approved by the local institutional review board. The 34 patients consisted of 25 men and 9 women, with a median age of 66 years (range, 41–85 years). Eight patients had recurrent tumors after surgical resection, and 26 patients had not received any previous treatment. The median clinical target volume was 510 cm^3.

Study Design

Imaging was performed before irradiation and at the end of treatment and then, in general, followed up at least every 12 months at our institution. For this study, we used magnetic resonance (MR) imaging as the main evaluation tool; however, if serial MR imaging could not be performed, a serial computed tomography (CT) was performed to replace MR imaging. In some patients, CT and MR imaging examinations were mixed during the follow-up period. For those patients, serial examinations performed with more regularity were adopted for this study. Magnetic resonance examination was performed with 1.5-T imagers (Magnetom Vision and Intera from Siemens, Erlangen, Germany, and Philips Medical Systems, Best, the Netherlands, respectively) with a phased array coil. The acquisition protocols were as follows: nonenhanced transverse turbo spin echo T1-weighted (620/13) and T2-weighted sequences (2300/90) with a slice thickness of 4 mm, an intersection gap of 1 mm, a field of view of 330 × 280 mm, and a matrix of 512 × 330, followed by fat-suppressed enhanced axial and sagittal T1-weighted sequences (620/13) with a slice thickness of 4 mm and an intersection gap of 1 mm after intravenous injection of 0.1 to 0.2 mmol/kg of gadopentetate dimeglumine (Magnevist; Schering, Berlin, Germany).

Computed tomographic examination was performed with a 16–detector row CT scanner (Sensation 16; Siemens). Our standardized CT scan protocol included an initial unenhanced scanning pass of the pelvis with a 0.75-mm collimation. This was followed by a contrast-enhanced pass with a 0.75-mm collimation 80 seconds after the start of an intravenous power injection of 100 mL of noniodinated material (iopamidol, Iopamiron 300; Bayer, Osaka, Japan) at 1.5 mL/s. The slice thickness of the MR and CT images was 5 mm.

We excluded from the study 8 patients with recurrence after resection. Another patient was excluded because her follow-up

was performed at the local hospital and we could not calculate the tumor volume. One patient who died of intercurrent disease within 1 year of the treatment was also excluded. Another patient was excluded because of multiple small skip lesions around the primary tumor site in the sacrum that were included in the original irradiated field during the first treatment. In this case, it was difficult to define the effectiveness of carbon ion radiotherapy for each lesion.

Analysis of Images for the Measurement of Tumor Volume

All procedures were conducted with the consensus of 3 authors from this study (R.I., T.K., and R.K.). T2-weighted imaging clearly delineated the chordomas from the surrounding tissue, allowing excellent assessment of the tumors. T2-weighted axial images were used to describe the region of interest with reference to T1-weighted and postcontrast T1-weighted axial images. In the evaluations by CT, postcontrast images were primarily used. In questionable cases, especially those with calcification and bone degeneration, both MR and CT images were used for reference, even if they were not examined at the same time. For quantification of the tumor volume, the tumor area on each tumor-containing section was delineated by an operator-defined region of interest, and the tumor volume was automatically calculated. In addition, the tumor volume ratio (VR) at each examination divided by the volume before irradiation was examined. For verification of tumor calcification, we used the latest CT images, which were taken at least 2 years after carbon ion radiotherapy. Computed tomographic images examined within 2 years were not regarded as appropriate for this assessment. We only compared the initial CT images with the last CT images. There were 14 patients who were candidates for the CT analysis.

Carbon Ion Radiotherapy

The specific techniques for carbon ion radiotherapy have been described in detail in previous reports.[6,9] The Heavy Ion Medical Accelerator in Chiba generates carbon ion beams. A carbon ion beam has the benefit of excellent dose distribution and better biological effectiveness compared with a photon beam. Tumors that are difficult to treat make good use of these advantages and are good controls.[5,6,9] For the definition of target volume, tumor spreading was estimated by MR, CT, and positron emission tomography. Carbon ion radiotherapy was performed once a day for 4 days a week (Tuesday to Friday), for a total of 16 fixed fractions in 4 weeks. A range of 2 to 4 irregularly shaped ports were applied, and 1 port was treated in each session. We used doses from 52.8 to 73.6 Gy equivalents (carbon physical dose [gray] multiplied by the relative biological effectiveness).[5,8] Relative biological effectiveness was evaluated by both radiobiological and physical studies.[7,9]

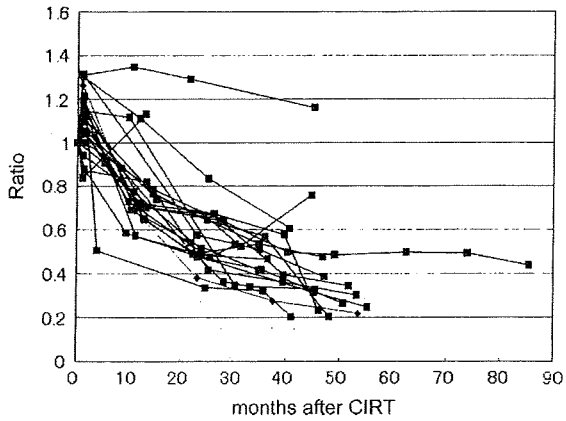

FIGURE 1. Changes in the tumor VR at the time of examination. The vertical axis indicates the tumor VR at each examination divided by the volume before irradiation, and the transverse axis is the number of months after carbon ion radiotherapy (CIRT). At the end of CIRT, temporary enlargement was observed in 13 cases.

TABLE 1. The Comparison of Tumor VR After CIRT (Cases)

	At the End of CIRT	Last Examination*
VR ≥ 1.1	13	1
1.1 > VR > 0.9	6	0
0.9 ≥ VR	4	20

*Excluding 2 recurrent cases.

Statistics

The follow-up period was calculated beginning from the initial date of carbon ion radiotherapy. The last follow-up date was on September 1, 2006. Local control and overall survival rates were calculated using the Kaplan-Meier method. The correlation between the tumor volume and the VR at the end of the treatment was tested. To assess tumor calcification changes, t test was used. All statistics were performed using Stat View 5.0 (SAS Institute Inc, Cary, NC). $P < 0.05$ was considered significant.

RESULTS

Treatment Results

Only 2 of the 34 patients in this study demonstrated local recurrence, 1 after 13 months and the other after 35 months. Four patients died because of disease, and another 4 died of intercurrent disease. The 5-year overall survival rate was 85.4%, and the 5-year local control rate was 93.8%.

Changes in Tumor Volume

Of the remaining 23 patients, including the 2 recurrent cases, 18 were examined by serial MR imaging and 5 by serial CT. Two patients did not have annual examinations, and we decided to add them to this analysis because their last images were obtained more than 2 years after carbon ion therapy, and we judged that using these images were appropriate for this study. By excluding the 2 recurrent cases, the median interval between the first and the last examinations was 46 months. The interval was longer than 3 years in 17 patients and between 2 and 3 years in 4 patients.

Figure 1 shows a plot of VR. At the end of the carbon ion radiotherapy, the VR had increased in most patients. The volume ratio at the end of the carbon ion radiotherapy was higher than 1.1 in 13 cases and lower than 0.9 in 4 cases (Table 1). In 12 of the 13 cases with a larger than 10% increase in size, continuous regression was observed after the initial enlargement. There was only 1 case in which the tumor volume did not revert back to the primary volume after the initial enlargement. The median VR was 0.36 in the last evaluation of 20 cases with decreasing size. In 4 cases, an enlargement larger than 20% of the initial volume occurred; however, at the time of the second examination, there was no continuous progression in size, and VR at the last evaluation was between 0.2 and 0.6 in 3 of the 4 cases and 1.16 in 1 case. The first regression of tumor volume to a ratio lower than 1.0 was observed between 1 and 25 months after carbon ion radiotherapy in 22 cases (Fig. 2).

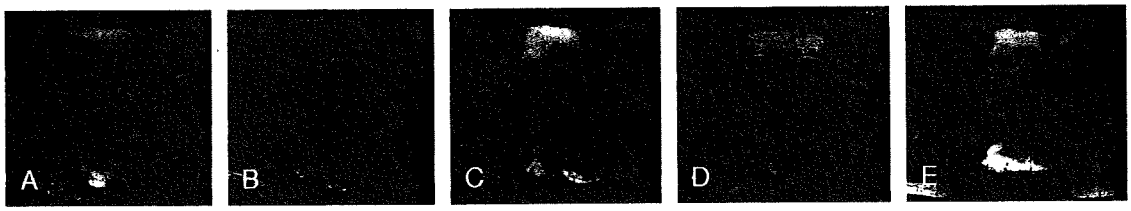

FIGURE 2. Serial axial T2-weighted images of sacral chordoma in a 61-year-old man. The tumor was temporary enlarged after carbon ion radiotherapy and then gradually shrank. A, Before carbon ion radiotherapy. B, At the end of carbon ion radiotherapy. C, Thirteen months after CIRT. D, Twenty-three months after CIRT. E, Forty-five months after CIRT.

We compared the annual mean VR in 11 available cases. We defined 1 year as occurring between 10 and 12 months after carbon ion radiotherapy, 2 years as 22 to 26 months, and 3 years as 34 to 38 months. The mean VR was 1.06, 0.72, 0.56, and 0.44, respectively, at the end of the carbon ion radiotherapy, and 1, 2, and 3 years, respectively, after the carbon ion radiotherapy.

Changes of Tumor Calcification

Tumor calcification was evaluated in 14 of the 23 cases by CT more than 2 years after carbon ion radiotherapy. Changes in tumor calcification were categorized into 3 patterns. The first was a pattern of calcification observed in tumors with both original bony structures, such as the sacral bone, and nonbony structures, such as where a tumor protrudes from the bone (n = 6; Fig. 3A). Another calcification pattern was observed in tumors with original bone structures only (n = 3; Fig. 3B). The third pattern consisted of areas where less calcification was observed in the tumor (n = 5; Fig. 3C). The extent of the pattern of calcification was not significantly correlated with the shrinkage ratio at the end of the treatment ($P = 0.5298$).

DISCUSSION

There have been few reports of sacral chordomas treated with modalities other than surgery because, before the appearance of carbon ion radiotherapy, only surgery could achieve long survival rates.[2–4,8] As we reported previously, carbon ion radiotherapy can achieve good results for sacral chordomas.[5] For this study, we made an effort to check the progress of our patients at least every 6 months; however, most of the candidates in this study were elderly and lived far from our hospital. Occasionally, our only recourse was to estimate a patient's tumor volume using imaging films taken at the local hospital, and we could not use such examinations as part of this study. Thus, there was some dispersion in the time when examinations for each patient were performed.

In 80% of the patients, we observed that tumors had increased or remained unchanged in size at the end of the carbon ion radiotherapy. It has been reported that the same phenomenon occurs in vestibular schwannomas after gamma knife radiotherapy.[10] In the study of schwannomas, 41% of the cases demonstrated temporary enlargement, and the local control rate was 81%. In a similar fashion, in our study, the tumor volume gradually decreased after initial enlargement. The tumor may enlarge owing to developing areas of necrosis and edema. Hemorrhage may also stimulate tumor growth that is often appearing as areas of high signal intensity on T1-weighted MR images. Nakamura et al[10] report that microsurgical resection of tumors show hyalinized thrombosis, thickening of the vascular wall, vascular obstruction, and granulomatous change, and this change help our inference. Even tumors with an enlargement larger than 20% demonstrated shrinkage upon the second examination. Considering these results, we could not conclude that recurrence would occur immediately upon observing initial enlargement. In 1 case, the tumor volume did not revert to the primary volume, but we did not confirm this change as recurrence because the tumor did not maintain a successive increase. Furthermore, the patient's symptoms were gradually relieved. Upon admission, he was bedridden with epidural anesthesia, but at the time of the last examination, he was active enough to maintain a part-time job.

In 4 cases, we observed that the tumor volume decreased lower than 10% and then rose higher than 10%. In 2 of these cases, a progressive increase in tumor volume was found by the local hospitals, and these were defined as local recurrence. One patient underwent CT examination after the last MR imaging. According to the findings of the last CT, regression of the tumor was apparent. In this case, the original tumor existed within the sacrum and did not protrude into the soft tissue around the sacrum. After treatment, calcification was observed to gradually accumulate in the soft part of the tumor on serial MR images. The last MR image revealed abnormal intensity, and the enhancement area by contrast medium was extended. The new CT examination performed did not reveal any apparent findings of local recurrence. It has been reported that radiation-induced insufficiency fractures show abnormal intensity on MR images.[11] Thus, we speculated that we misunderstood the abnormal intensity on the MR images caused by calcification change and degeneration of sacral bone as tumor spreading. In the other case, a compression fracture in the sacral bone occurred 2 years after carbon ion radiotherapy. Owing to the bone degeneration and misalignment caused by the fracture,

FIGURE 3. Changes of tumor calcification. A, Calcification in the tumor in both the original bony structures, such as the sacral bone, and the nonbony structures, such as where the tumor protruded from the bone. B, Calcification in the tumor in only the original bony structure. C, Less calcification in the tumor.

abnormal intensity was seen on the MR images, and we confused this abnormality with tumor spreading. For cases such as these, images from another axis of the body or a combination of several modalities would be useful. Except in cases of recurrence, sequential enlargement was generally not observed, and to judge recurrence, we will need to monitor regrowth 2 or more times in a row.

Regarding the relationship between tumor volume and tumor regression, the rate of regression at the end of carbon ion radiotherapy was not significantly correlated with the initial tumor volume. We could not speculate on the speed of shrinkage by considering the initial volume. The accumulation level of calcification was not significantly related to the initial ratio of regression. As for the prediction of local control, only 2 patients in this study had local recurrence, and it was hard to determine a relationship between recurrence and reaction to carbon ion radiotherapy.

In cases where the tumor volume has not decreased or there are residual findings on CT and MR images, to know whether tumor regression will occur is important for orthopedic surgeons referring patients. This data could indicate whether chordomas treated with carbon ion radiotherapy had sufficient potential to become reduced in size during observation. We suggest a waiting period and frequent monitoring of follow-up imagings before diagnosing cases of recurrence, unless symptoms deteriorate or the tumor continuously enlarges. Carbon ion radiotherapy does not have a long history, but we have been able to use it to treat a growing number of cases of chordoma. Chordoma is a slow-growing tumor that requires a long follow-up period, and a large number of cases are needed to establish the efficacy of carbon ion radiotherapy. However, we believe that carbon ion radiotherapy is an effective local treatment of chordoma.

ACKNOWLEDGMENTS

The authors thank Hisao Ito, MD, PhD, Department of Radiology, Chiba University Hospital.

REFERENCES

1. Sundaresan N. Chordomas. *Clin Orthop Relat Res.* 1986;204:135–142.
2. York JE, Kaczaraj A, Abi-Said D, et al. Sacral chordoma: 40-year experience at a major cancer center. *Neurosurgery.* 1999;44:74–79.
3. Catton C, O'Sullivan B, Bell R, et al. Chordoma: long-term follow-up after radical photon irradiation. *Radiother Oncol.* 1996;41:67–72.
4. Ozaki T, Hillmann A, Winkelmann W. Surgical treatment of sacrococcygeal chordoma. *J Surg Oncol.* 1997;64:274–279.
5. Imai R, Kamada T, Tsuji H, et al. Carbon ion radiotherapy for unresectable sacral chordomas. *Clin Cancer Res.* 2004;10:5741–5746.
6. Kamada T, Tsujii H, Tsuji H, et al. Efficacy and safety of carbon ion radiotherapy in bone and soft tissue sarcomas. *J Clin Oncol.* 2002; 20:4466–4471.
7. Kanai T, Endo M, Minohara S, et al. Biophysical characteristics of HIMAC clinical irradiation system for heavy-ion radiation therapy. *Int J Radiat Oncol Biol Phys.* 1999;44:201–210.
8. Fuller DB, Bloom J. Radiotherapy for chordoma. *Int J Radiat Oncol Biol Phys.*1988;15:331–339.
9. Tsujii H, Mizoe JE, Kamada T, et al. Overview of clinical experiences on carbon ion radiotherapy at NIRS. *Radiother Oncol.* 2004;73:S41–49.
10. Nakamura H, Jokura H, Takahashi K, et al. Serial follow-up MR imaging after gamma knife radiosurgery for vestibular schwannoma. *Am J Neuroradiol.* 2000;21:1540–1546.
11. Blomlie V, Rofstad EK, Talle K, et al. Incidence of radiation-induced insufficiency fractures of the female pelvis: evaluation with MR imaging. *Am J Roentgenol.* 1996;167:1205–1210.

Radiotherapy and Oncology 92 (2009) 231–237

Contents lists available at ScienceDirect

Radiotherapy and Oncology

journal homepage: www.thegreenjournal.com

Radiotherapy of pancreatic cancer

Four-dimensional measurement of intrafractional respiratory motion of pancreatic tumors using a 256 multi-slice CT scanner

Shinichiro Mori [a,*], Ryusuke Hara [a], Takeshi Yanagi [a], Gregory C. Sharp [b], Motoki Kumagai [a], Hiroshi Asakura [c], Riwa Kishimoto [a], Shigeru Yamada [a], Susumu Kandatsu [a], Tadashi Kamada [a]

[a] Research Center for Charged Particle Therapy, National Institute of Radiological Sciences, Chiba, Japan
[b] Department of Radiation Oncology, Massachusetts General Hospital, USA
[c] Accelerator Engineering Corporation, Chiba, Japan

ARTICLE INFO

Article history:
Received 26 July 2008
Received in revised form 4 December 2008
Accepted 7 December 2008
Available online 9 February 2009

Keywords:
Carbon beam
CT
Four-dimensional
Pancreas
Radiation therapy

ABSTRACT

Purpose: To quantify pancreas and pancreatic tumor movement due to respiratory motion using volumetric cine CT images.
Materials and methods: Six patients with pancreatic tumors were scanned in cine mode with a 256 multi-slice CT scanner under free breathing conditions. Gross tumor volume (GTV) and pancreas were manually contoured on the CT data set by a radiation oncologist. Intrafractional respiratory movement of the GTV and pancreas was calculated, and the results were compared between the respiratory ungated and gated phases, which is a 30% duty cycle around exhalation.
Results: Respiratory-induced organ motion was observed mainly in the anterior abdominal side than the posterior side. Average GTV displacement (ungated/gated phases) was 0.7 mm/0.2 mm in both the left and right directions, and 2.5 mm/0.9 mm in the anterior, 0.1 mm/0 mm in the posterior, and 8.9 mm/2.6 mm in the inferior directions. Average pancreas center of mass displacement relative to that at peak exhalation was mainly in the inferior direction, at 9.6 mm in the ungated phase and 2.3 mm in the gated phase.
Conclusions: By allowing accurate determination of the margin, quantitative analysis of tumor and pancreas displacement provides useful information in treatment planning in all radiation approaches for pancreatic tumors.
 Radiotherapy and Oncology 92 (2009) 231–237

Organ motion due to respiration has been investigated using a variety of methods, including fluoroscopy, ultrasound (US), MRI, CT and PET, in the lung [1–6], liver [7–10], pancreas [11,12], kidney, and prostate sites. An understanding of motion characteristics in radiotherapy planning is useful in determining internal margin and optimizing beam parameters (beam angle etc.), because the degradation of image quality due to respiratory motion affects radiotherapy planning and delivery of the treatment beam.

However, quantification of organ motion using a single two-dimensional projection image limits the information which can be captured to out-of-plane motion, rotation or deformation during breathing. This is because tumors moving under respiration do not behave consistently, but rather move in different paths during inhalation and exhalation in a hysteresis-like manner. In the abdominal region, recently introduced CT scanners can acquire respiratory-correlated volumetric images (four-dimensional CT: 4DCT), thus allowing the direct observation of several points (3D) of movement. However, a fundamental problem with 4DCT is that the images obtained by conventional multi-slice CT need to be resorted in the same respiratory phase, because even the latest commercially available multi-slice CT scanners obtain less than 4 cm in a single rotation. As a result, images in patients with low reproducibility of respiratory motion or irregular breathing may be subjected to image sorting errors and degraded image quality.

We have developed a 256 multi-slice CT scanner, which allows volumetric cine imaging without the resorting process required with conventional 4DCT scanners. This is achieved simply by extending the scan coverage of a commercially available multi-slice CT scanner to provide wide scan coverage in a single rotation with high spatiotemporal resolution (see Materials and method). The 256 multi-slice CT improves image quality in 4D imaging with a coherent time axis in all slices.

Given the presence of critical organs around the pancreas such as the duodenum, beam overshoot or undershoot due to respiratory motion may increase patient risk. To our knowledge, however, a quantitative four-dimensional analysis of pancreas respiratory movement using 4DCT data sets has not been reported.

* Corresponding author. Address: Research Center for Charged Particle Therapy, National Institute of Radiological Sciences, Inage-ku, Chiba 263-8555, Japan.
E-mail address: shinshin@nirs.go.jp (S. Mori).

0167-8140/$ - see front matter © 2009 Elsevier Ireland Ltd. All rights reserved.
doi:10.1016/j.radonc.2008.12.015

Here, we evaluated pancreas and pancreatic tumor movement due to respiratory motion using the 256 multi-slice CT scanner.

Materials and methods

Patient and data acquisition

Six inpatients were selected from a group of patients with pancreatic tumors (mean age: 60.6 y, SD ±6.4 y) treated with carbon beam radiotherapy for adenocarcinoma of the pancreas. Each patient consented to participate in the study, which was approved by the Institutional Review Board for human research of the National Institute of Radiological Sciences (NIRS). Patient characteristics and tumor size are summarized in Table 1.

After a 10-min rest in the supine position on the CT bed, CT scans were performed using the 256 multi-slice CT in cine mode, which was developed by the NIRS and Toshiba Medical Systems as a prototype for a commercially available 320 multi-slice CT (Aquilion One, Toshiba Medical Systems, Otawara, Japan) [13–15]. SI coverage is 128 mm per rotation. Patients were fixed on the patient bed with immobilization, as routinely used in treatment. Scan conditions were slice collimation of 128 × 1.0 mm, 0.5 s in a single rotation and scan time of less than 6 s to obtain one respiratory cycle without patient couch movement. Scans were performed under free breathing conditions with a respiratory sensing monitor, which consists of a PSD (position-sensitive detector) sensor and an infrared-emitting light termed an "active" marker [16] (Toyonaka Lab, Osaka, Japan). The respiratory signal is transferred to the CT console and recorded in the CT projection data via an ECG signal input connector. This process removes any delay in synchronizing between the respiratory signal and reconstructed CT images. The respiratory cycle was subdivided into 10 phases by selecting peak inhalation (T0) and peak exhalation (T50) based on the amplitude of the respiratory signal, and the respiratory phases are therefore not equidistant. This division method is more consistent with the phase-based sorting method used in clinical situations.

As described above, the 256 multi-slice CT scanner does not require the image resorting for respiratory phase required for 4DCT of the relevant anatomy at specific respiratory phases, as is done in conventional MSCT. This is because the 4DCT artifacts (banding artifacts or missing slices) typically observed with conventional MSCT [17] do not occur with the 256 multi-slice CT scanner [5,18], as they are minimized by the absolute time stamp without data sorting in the 256 multi-slice CT. We therefore define the CT data sets obtained by the 256 multi-slice CT as volumetric cine data in this paper.

Data analysis

Two metrics were evaluated using volumetric cine data: (1) intrafractional respiratory movement of the GTV and (2) pancreas. These metrics were compared between a single respiratory cycle (respiratory ungated phase) and 30% duty cycle around peak exhalation (respiratory gated phase), which were calculated using volumetric cine data sets for the whole respiratory cycle (T0–T90) and around the exhalation phase (T40–T60), respectively.

The GTV and pancreas were manually contoured on the CT data set at peak exhalation by a certified radiation oncologist who had more than 10 years clinical experience (R.H. or T.Y.). Both contours at other respiratory phases were calculated by B-spine based deformable registration [19], following which the oncologist checked the contour curves in axial, coronal and sagittal sections at each phase, and takes less than 15 min for phase to phase using a single CPU (central processing unit). Although most cases did not require changes to contours, we did make minor changes when gas bowel motion was observed. The overall accuracy of contours was considered clinically acceptable.

The GTV center of mass (COM) trajectory at each respiratory phase was calculated, and IM (internal margin) was calculated as the distance from the edge of the tumor at peak exhalation to that at a certain respiratory phase (Fig. 1a). For evaluation of the pancreas, we calculated COM and moving distance at the pancreas head, body and tail (described as P_{head}, P_{body} and P_{tail} in Fig. 1b) as a function of respiratory phase.

Results

Sagittal volumetric cine images with GTV contour curves are shown in Fig. 2 (patient no. 5). To clarify intrafractional motion, a blue mesh grid was set on the CT image at peak exhalation (T50). 3D deformable analysis was done from peak exhalation in each respiratory phase, and then the results were applied to the mesh grid on the CT data at each respiratory phase. Results showed that respiratory-induced organ motion occurred mainly at the anterior abdominal aspect rather than the posterior side. Bowel gas also moved as a function of time, but this movement was not reproducible. The GTV shape is deformed as a function of respiratory phase by movement of the anterior side of the GTV in an inferior direction to a greater degree than that of its posterior side.

The GTV COM in this patient moved 0.8 mm/0.7 mm (left/right side), 0.5 mm/0.4 mm (anterior/posterior side) and 0 mm/8.2 mm (superior/inferior side) in the ungated phase, and 0.5 mm/0.7 mm (left/right side), 0.4 mm/0 mm (anterior/posterior side) and 0 mm/2.6 mm (superior/inferior side) in the gated phase. The GTV COM moved in the SI direction, mainly due to intrafractional respiratory motion.

Fig. 3 shows GTV-COM displacement for all patients, with peak inhalation (T0) and peak exhalation (T50) indicated by solid circles. Most tumors moved in a varying orbit during the respiratory cycle in a hysteresis-like manner. This characteristic is useful in determining margins. For all patients, average COM displacement for the ungated phase relative to that at peak exhalation was 0.7 mm in both the left and right directions, and 2.5 mm in the anterior, 0.1 mm in the posterior and 8.9 mm in the inferior directions. In contrast, average COM displacement in the gated phase

Table 1
Patient characteristics.

Pt. no.	Age (y)[a]	Sex	T-stage		Pathologic type	GTV size (cm) (LR × AP × SI)	Location
1	67	M	cT4N0M0	4	Adenocarcinoma	9.8 × 4.8 × 2.9	Pancreas body
2	80	F	T4N0M0	4	Adenocarcinoma	5.4 × 4.1 × 3.6	Pancreas head
3	46	M	cT4N0M0	4	Adenocarcinoma	5.4 × 5.4 × 4.4	Pancreas body–tail
4	64	F	cT4N0M0	4	Adenocarcinoma	6.2 × 3.4 × 2.5	Pancreas head
5	48	M	cT4N0M0	4	Adenocarcinoma	6.3 × 4.8 × 3.5	Pancreas head
6	63	M	T4N2M0	4	Adenocarcinoma	9.1 × 6.3 × 4.0	Pancreas tail

Abbreviations: COM, center of mass; Pt. no., patient number; LR, left–right; AP, anterior–posterior; SI, superior–inferior.
[a] Mean ± SD, 61.3 ± 12.7 y.

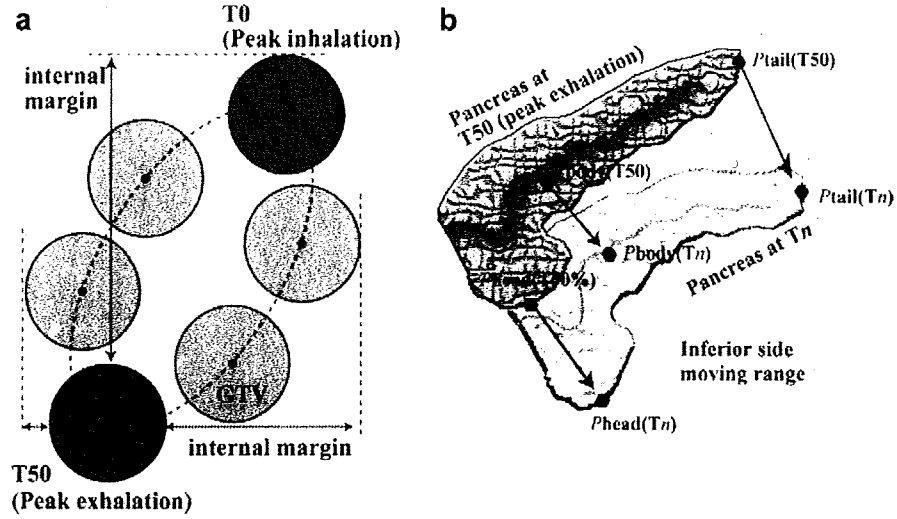

Fig. 1. Schematic drawing of (a) GTV displacement and internal margin in one respiratory cycle and (b) respiratory movement range for the pancreas between peak exhalation (T50) and a certain phase (*Tn*).

was minimized to 0.9 mm in the anterior and 2.6 mm in the inferior directions, and close to 0.0 mm in the other directions. Results are summarized in Table 2.

From these results, the average margin added to the GTV at peak exhalation was 0.2 mm/0.5 mm (left/right side), 2.6 mm/0.2 mm (anterior/posterior side) and 0.3 mm/9.5 mm (superior/inferior side) for the ungated phase, compared with 0.0 mm/0.0 mm (right/left), 0.8 mm/0.2 mm (anterior/posterior side) and 0.3 mm/3.0 mm (superior/inferior side) in the gated phase.

With regard to movement of the pancreas, 3D visualization of the pancreas COM for all patients is shown in Fig. 4. The main COM displacement was in the SI direction, although AP movements

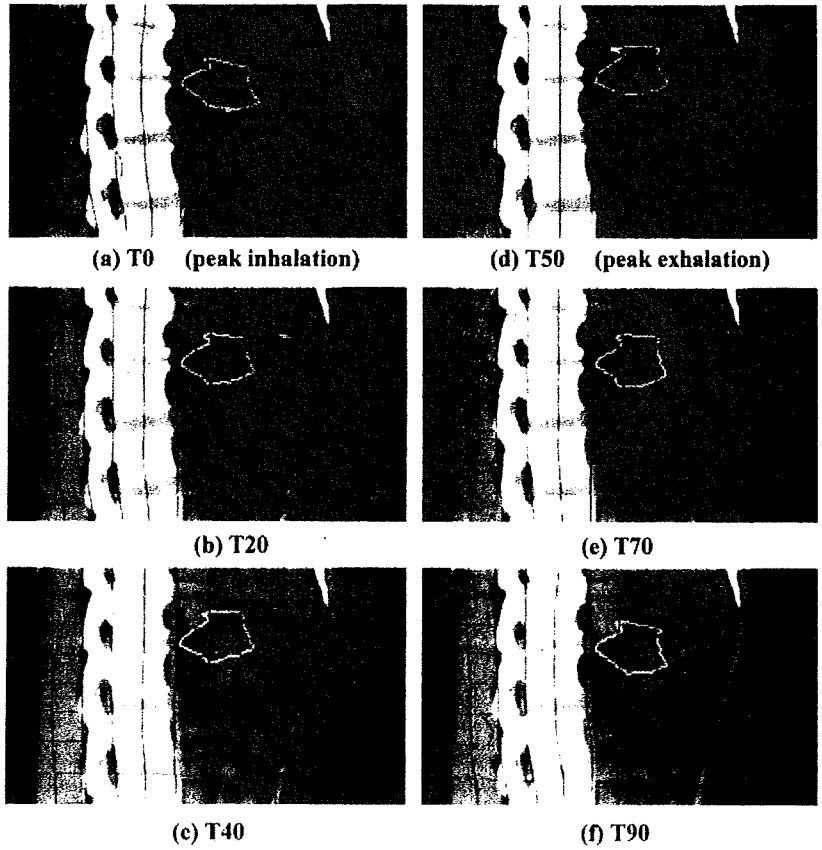

Fig. 2. Four-dimensional sagittal CT images (patient no 5). (a) T0 (peak inhalation), (b) T20, (c) T40, (d) T50 (peak exhalation), (e) T70 and (f) T90. The yellow line and blue mesh grid show the GTV contours and deformed space from peak exhalation, respectively.

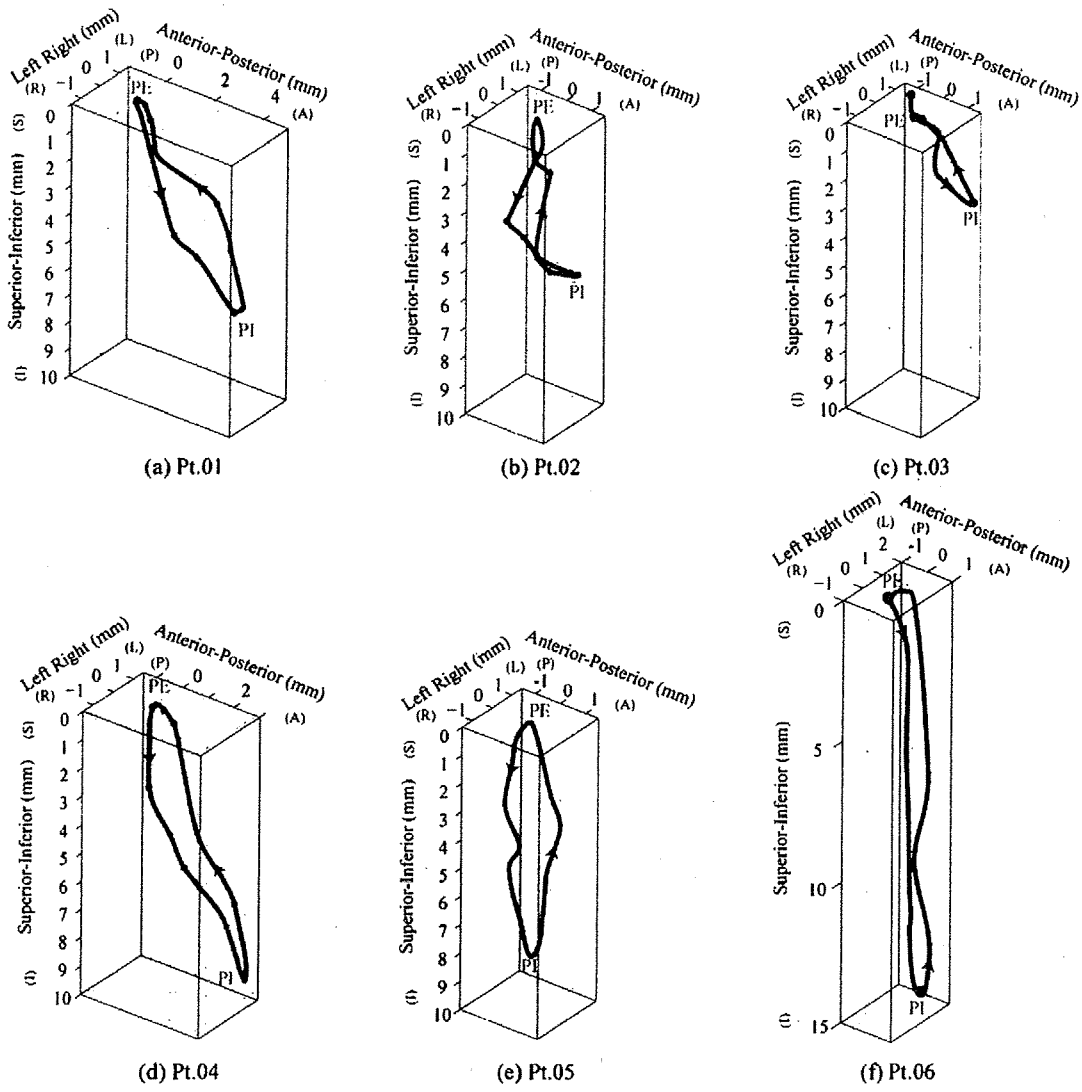

Fig. 3. 3D visualization of tumor center of mass (COM) displacement. Respiratory cycle and distance between PE (peak exhalation) and PI (peak inhalation) are shown in parentheses. *Abbreviations:* L, left; R, right; A, anterior; P, posterior; S, superior; I, inferior.

of a few millimeters were also observed. Pancreas COM displacement in the inferior direction was 8.2 and 2.6 mm in the ungated and gated phases, respectively. The magnitude of geometrical variation increased with greater approximation to the inhalation phase. Further, geometrical variation was greater around the pancreas tail than the pancreas body and head regions (Fig. 4).

For all patients, average pancreas COM displacement relative to that at peak exhalation was mainly in the inferior direction, at

Table 2
Average GTV center of mass displacement and margin added to the GTV at peak exhalation between peak inhalation (T0) and peak exhalation (T50).

Metrics	Strategy		Left	Right	Anterior	Posterior	Superior	Inferior
COM	Ungated	Mean	0.7	0.7	2.5	0.1	0.0	8.9
		Range	0.3–1.0	0.0–1.7	0.5–4.4	0.0–0.4	0.0–0.2	3.7–14.5
		SD	0.3	0.6	1.4	0.2	0.1	3.8
	Gated	Mean	0.2	0.3	0.9	0.0	0.0	2.6
		Range	0.0–0.5	0.0–0.7	0.0–2.0	0.0–0.3	0.0–0.2	0.7–5.9
		SD	0.2	0.3	0.7	0.1	0.1	1.8
Margin	Ungated	Mean	0.2	0.5	2.6	0.2	0.3	9.5
		Range	0.0–0 8	0.0–3.1	0.6–4.7	0.0–1.3	0.0–20	6.0–12.0
		SD	0.4	1.3	1.3	0.5	0.8	2.3
	Gated	Mean	0.0	0.0	0.8	0.2	0.3	3.0
		Range	0.0–0.0	0.0–0.0	0.0–3.1	0.0–1.3	0.0–2.0	1.0–6.0
		SD	0.0	0.0	1.3	0.5	0.8	1.7

Unit: mm.
Abbreviations: COM, center of mass; SD, standard deviation.

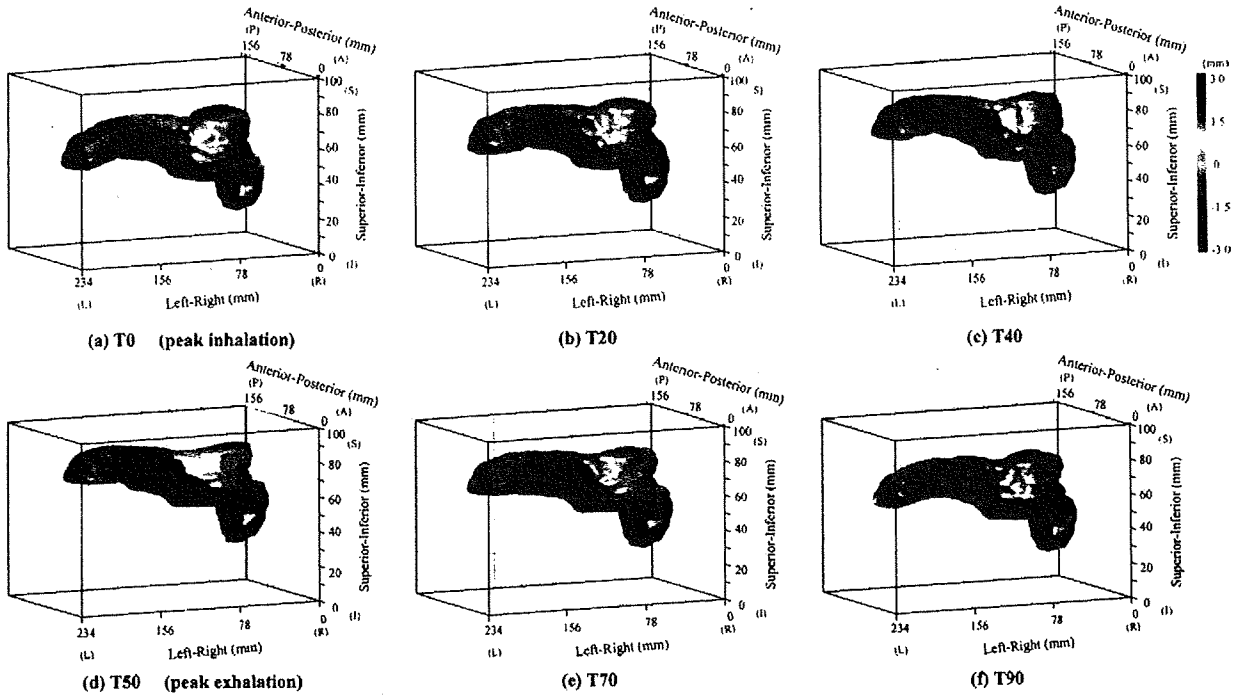

Fig. 4. 3D-visualized pancreas and the magnitude of geometrical variation from peak exhalation as a function of respiratory phase (patient no 5). (a) T0 (peak inhalation), (b) T20, (c) T40, (d) T50 (peak exhalation), (e) T70 and (f) T90.

9.6 mm for the ungated phase and 2.3 mm for the gated phase. The results are summarized in Table 3.

Pancreas head, body and tail displacement as a function of respiratory phase is visualized as a 3D plot in Fig. 5. The average pancreas head, body and tail displacement in the inferior direction for the ungated phase was 8.3, 9.6 and 13.4 mm, respectively, which was minimized in the gated phase to 2.8, 2.8 and 3.6 mm, respectively. Displacement of the pancreas tail was greater than that of the others.

Discussion

In this study, we quantified respiratory-induced movement of the pancreas tumor and pancreas using volumetric cine CT data sets and found that the significant decrease in margin in the gated phase may be useful in minimizing excessive doses to normal tissues during radiotherapy.

In the thoracic region, the high contrast of lung tumors against the lung allows the direct observation of tumor motion

Table 3
Average pancreas center of mass displacement and moving distance in the pancreas head; body and tail between peak inhalation (T0) and peak exhalation (T50).

Metrics	Strategy		Left	Right	Anterior	Posterior	Superior	Inferior
COM	Ungated	Mean	1.6	0.6	2.0	0.7	0.2	9.6
		Range	0.0–4.7	0.0–2.7	0.3–3.4	0.0–3.0	0.0–1.1	5.8–14.7
		SD	1.8	1.1	1.2	1.2	0.4	3.3
	Gated	Mean	0.9	0.6	0.6	0.3	0.2	2.3
		Range	0.0–2.6	0.0–2.7	0.0–1.2	0.0–0.7	0.0–1.1	0.8–3.9
		SD	1.0	1.1	0.5	0.3	0.4	1.2
Pancreas head	Ungated	Mean	2.7	0.1	2.4	0.3	0.0	8.3
		Range	0.9–3.8	0.0–0.7	0.7–4.1	0.0–1.0	0.0–0.0	6.9–9.5
		SD	1.0	0.3	1.3	0.5	0.0	0.9
	Gated	Mean	1.1	0.1	0.9	0.1	0.0	2.8
		Range	0.5–1.9	0.0–0.3	0.6–1.6	0.0–0.7	0.0–0.0	0.5–4.0
		SD	0.6	0.1	0.4	0.3	0.0	1.3
Pancreas body	Ungated	Mean	1.8	2.5	2.4	1.2	0.0	9.6
		Range	0.0–8.5	0.1–6.1	1.0–4.6	0.0–4.2	0.0–0.0	5.2–12.5
		SD	3.3	2.2	1.7	1.6	0.0	2.5
	Gated	Mean	0.9	2.3	1.4	0.5	0.0	2.8
		Max	0.0–3.2	0.0–6.1	1.0–2.9	0.0–1.2	0.0–0.0	0.5–6.3
		SD	1.2	2.4	0.8	0.5	0.0	2.0
Pancreas tail	Ungated	Mean	1.7	0.9	1.6	1.2	0.1	13.4
		Range	0.3–3.0	0.0–2.8	0.4–3.6	0.0–4.9	0.0–0.5	8.5–16.7
		SD	0.9	1.2	1.4	1.8	0.2	3.8
	Gated	Mean	0.7	0.5	0.6	0.6	0.1	3.6
		Range	0.0–1.3	0.0–2.0	0.0–2.2	0.0–0.8	0.0–0.5	1.5–9.5
		SD	0.4	0.8	0.9	0.3	0.2	2.9

Unit: mm.
Abbreviations: COM, center of mass; SD, standard deviation.

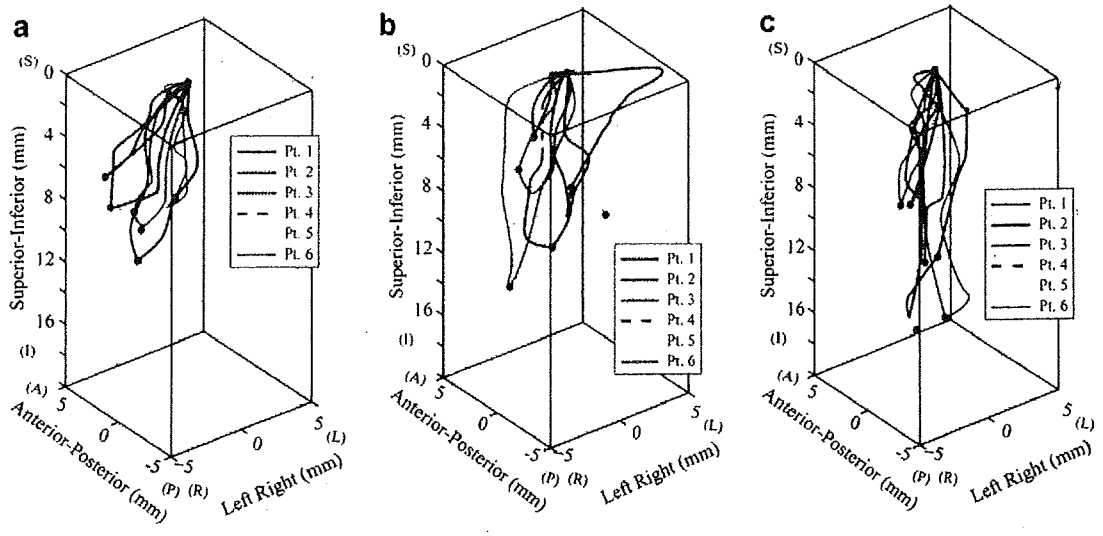

Fig. 5. 3D visualization of (a) pancreas head, (b) pancreas body and (c) pancreas tail trajectories for all patients. Respiratory cycle and distance between PE and PI are shown in parentheses.

on fluoroscopic imaging. In the abdominal region, however, owing to the usually weak contrast between tumor and normal tissues, standard practice is to use an artificial marker to track tumor displacement, or US, etc. In their evaluations of pancreatic movement using US, Suramo et al. [12] and Byran et al. [11] reported displacement in the SI direction of approximately 2 cm (range: 0–3 cm) under free breathing conditions [20]. Moustakis et al. evaluated pancreas positional variation under breath-holding conditions using multi-phase contrast-enhanced spiral CT scans, and reported that the most mobile part of the pancreas was the pancreatic tail [21]. Although their study did not use 4DCT, our present study also found that the most mobile part of the pancreas under free breathing conditions was the pancreatic tail.

We used volumetric cine CT images to clearly visualize pancreatic movement as 3D trajectory plus time and the magnitude of deformation, allowing us to quantify 3D displacement of the pancreatic tumor and pancreas and thereby to define the necessary margins for radiotherapy in the respiratory ungated/gated phases. Our volumetric cine CT data have high spatiotemporal resolution (slice thickness of 1.0 mm and 0.5 s per single rotation), resorting of CT images is not necessary, and the 4DCT artifacts as observed in conventional multi-slice CT do not occur. As described in Materials and methods, the accuracy of our results, including deformable registration, is much improved over those obtained using conventional CT. Moreover, we also observed bowel gas movement with accurate geometrical shape as a function of time. Although visualization of reproducible motion such as respiration and heart beat on CT images using a conventional multi-slice CT is feasible, that of transient motion such as of bowel gas is not. These characteristics highlight the advantages of the 256 multi-slice CT in volumetric cine imaging over existing multi-slice CTs.

In this study, we focused on the four-dimensional evaluation of GTV and pancreas movement, not on dose calculation in radiotherapy. Nevertheless, thanks to their accurate definition of internal margin and treatment strategy (respiratory ungated/gated phase), our results may be useful in dose calculation. In particular, radiotherapy in our institute is performed using heavy charged particle beams (= carbon ion beam), the characteristics of which are distinctly different from those of photon beams. Charged particles have a finite range in tissue and deposit most of their energy just before stopping (Bragg peak) [22], allowing the delivery of a higher dose to the target region only. For this reason, inaccurate target definition using the internal margin may increase harmful dosage to normal tissues more strongly than is possible with photon beams, because the beam stopping position in charged particle therapy is sensitive to 'geometrical' rather than 'radiological' pathlength. The magnitude of radiological pathlength variation might therefore cause overdosing to normal tissues and underdosing to the tumor. Our institute is now constructing a new facility for carbon beam scanning treatment [23], which should allow a greater decrease in dose conformation in scanning irradiation than is possible with conventional passive beam irradiation [24].

Several limitations of this study warrant discussion. Because we evaluated pancreas and pancreatic tumor movement and the resulting necessary margins using only single respiratory cycle 4DCT, our evaluation is based on the implicit assumption that the respiratory trace is reproducible at treatment. Moreover, the definition of the gating window is a trade-off between the amount of residual motion and duty cycle. In this study, the amplitude-based definition of the gating window as a 30% duty cycle around exhalation (±10% from peak exhalation (= T50)) represents a good balance between the amount of residual motion and duty cycle.

Some researchers have reported the occurrence of interfractional tumor positional changes [25,26], which are described as changes in tumor position between individual treatment fractions. Margin definition should therefore be done with due consideration to the time span between the 4DCT scan and treatment, and account for motion that is not captured during 4DCT.

Conclusion

Volumetric cine CT significantly improves the observation of organ and tumor displacement, and overcomes some of the limitations of present CT methods. The pancreas and pancreatic tumors move mainly in an inferior direction, but also show several millimeters' movement in the anterior direction, which cannot be neglected. Proper analysis of the respiratory gated phase can significantly reduce the margin of the GTV. Moreover, owing to its accurate determination of the margin, volumetric cine scanning is a useful complement to current irradiation methods. Although a limited number of patients were evaluated in this study, we believe that our initial analysis and results using the 256 multi-slice CT scanner will be highly useful to the radiotherapy community and will help improve pancreatic cancer treatment using charged particle beam as well as photon beam.

References

[1] Engelsman M, Damen EM, De Jaeger K, et al. The effect of breathing and set-up errors on the cumulative dose to a lung tumor. Radiother Oncol 2001;60:95–105.

[2] Grills IS, Yan D, Martinez AA, et al. Potential for reduced toxicity and dose escalation in the treatment of inoperable non-small-cell lung cancer: a comparison of intensity-modulated radiation therapy (IMRT), 3D conformal radiation, and elective nodal irradiation. Int J Radiat Oncol Biol Phys 2003;57:875–90.

[3] Hanley J, Debois MM, Mah D, et al. Deep inspiration breath-hold technique for lung tumors: the potential value of target immobilization and reduced lung density in dose escalation. Int J Radiat Oncol Biol Phys 1999;45:603–11.

[4] Kubo HD, Hill BC. Respiration gated radiotherapy treatment: a technical study. Phys Med Biol 1996;41:83–91.

[5] Mori S, Endo M, Komatsu S, et al. Four-dimensional measurement of lung tumor displacement using 256-multi-slice CT-scanner. Lung Cancer 2007;56:59–67.

[6] Stevens CW, Munden RF, Forster KM, et al. Respiratory-driven lung tumor motion is independent of tumor size, tumor location, and pulmonary function. Int J Radiat Oncol Biol Phys 2001;51:62–8.

[7] Balter JM, Ten Haken RK, Lawrence TS, et al. Uncertainties in CT-based radiation therapy treatment planning associated with patient breathing. Int J Radiat Oncol Biol Phys 1996;36:167–74.

[8] Shimizu S, Shirato H, Xo B, et al. Three-dimensional movement of a liver tumor detected by high-speed magnetic resonance imaging. Radiother Oncol 1999;50:367–70.

[9] Weiss PH, Baker JM, Potchen EJ. Assessment of hepatic respiratory excursion. J Nucl Med 1972;13:758–9.

[10] Davies SC, Hill AC, Holmes RB, et al. Ultrasound quantitation of respiratory organ motion in the upper abdomen. Br J Radiol 1994;67:1096–102.

[11] Bryan P, Custar S, Haaga J, et al. Respiratory movement of the pancreas: an ultrasonic study. J Ultrasound Med 1984;3:317–20.

[12] Suramo I, Paivansalo M, Myllyla V. Cranio-caudal movements of the liver, pancreas and kidneys in respiration. Acta Radiol Diagn (Stockh) 1984;25:129–31.

[13] Endo M, Mori S, Tsunoo T, et al. Development and performance evaluation of the first model of 4D CT-scanner. IEEE Trans Nucl Sci 2003;50:1667–71.

[14] Mori S, Endo M, Tsunoo T, et al. Physical performance evaluation of a 256-slice CT-scanner for four-dimensional imaging. Med Phys 2004;31:1348–56.

[15] Endo M, Mori S, Kandatsu S, et al. Development and performance evaluation of the second model 256-detector row CT. Radiol Phys Technol 2008;1:20–6.

[16] Minohara S, Kanai T, Endo M, et al. Respiratory gated irradiation system for heavy-ion radiotherapy. Int J Radiat Oncol Biol Phys 2000;47:1097–103.

[17] Yamamoto T, Langner U, Loo Jr BW, et al. Retrospective analysis of artifacts in four-dimensional CT images of 50 abdominal and thoracic radiotherapy patients. Int J Radiat Oncol Biol Phys 2008;72:1250–8.

[18] Mori S, Endo M, Kohno R, et al. Respiratory correlated segment reconstruction algorithm towards four-dimensional radiation therapy using carbon ion beams. Radiother Oncol 2006;80:341–8.

[19] Wu Z, Rietzel E, Boldea V, et al. Evaluation of deformable registration of patient lung 4DCT with subanatomical region segmentations. Med Phys 2008;35:775–81.

[20] Keall PJ, Mageras GS, Balter JM, et al. The management of respiratory motion in radiation oncology report of AAPM Task Group 76. Med Phys 2006;33:3874–900.

[21] Horst E, Micke O, Moustakis C, et al. Conformal therapy for pancreatic cancer: variation of organ position due to gastrointestinal distention – implications for treatment planning. Radiology 2002;222:681–6.

[22] Bragg WH, Kleeman R. On the ionisation curves of radium. Phil Mag 1904;8:726–38.

[23] Noda K, Furukawa T, Fujisawa T, et al. New accelerator facility for carbon-ion cancer-therapy. J Radiat Res (Tokyo) 2007;48(Suppl. A):A43–54.

[24] Furukawa T, Inaniwa T, Sato S, et al. Design study of a raster scanning system for moving target irradiation in heavy-ion radiotherapy. Med Phys 2007;34:1085–97.

[25] Korreman SS, Juhler-Nottrup T, Boyer AL. Respiratory gated beam delivery cannot facilitate margin reduction, unless combined with respiratory correlated image guidance. Radiother Oncol 2008;86:61–8.

[26] Britton KR, Starkschall G, Tucker SL, et al. Assessment of gross tumor volume regression and motion changes during radiotherapy for non-small-cell lung cancer as measured by four-dimensional computed tomography. Int J Radiat Oncol Biol Phys 2007;68:1036–46.

Int. J. Radiation Oncology Biol. Phys., Vol. 76, No. 1, pp. 303–312, 2010

0360-3016/10/$–see front matter

ELSEVIER

doi:10.1016/j.ijrobp.2009.05.026

PHYSICS CONTRIBUTION

COMPARISON OF RESPIRATORY-GATED AND RESPIRATORY-UNGATED PLANNING IN SCATTERED CARBON ION BEAM TREATMENT OF THE PANCREAS USING FOUR-DIMENSIONAL COMPUTED TOMOGRAPHY

SHINICHIRO MORI, PH.D.,* TAKESHI YANAGI, M.D.,* RYUSUKE HARA, M.D.,* GREGORY C. SHARP, PH.D.,† HIROSHI ASAKURA, M.S.,‡ MOTOKI KUMAGAI, M.S.,* RIWA KISHIMOTO, M.D.,* SHIGERU YAMADA, M.D.,* HIROTOSHI KATO, M.D.,* SUSUMU KANDATSU, M.D.,* AND TADASHI KAMADA, M.D.*

*Research Center for Charged Particle Therapy, National Institute of Radiological Sciences, Chiba, Japan; †Department of Radiation Oncology, Massachusetts General Hospital, and Harvard Medical School, Boston, Massachusetts; and ‡Accelerator Engineering Corporation, Chiba, Japan

Purpose: We compared respiratory-gated and respiratory-ungated treatment strategies using four-dimensional (4D) scattered carbon ion beam distribution in pancreatic 4D computed tomography (CT) datasets.
Methods and Materials: Seven inpatients with pancreatic tumors underwent 4DCT scanning under free-breathing conditions using a rapidly rotating cone-beam CT, which was integrated with a 256-slice detector, in cine mode. Two types of bolus for gated and ungated treatment were designed to cover the planning target volume (PTV) using 4DCT datasets in a 30% duty cycle around exhalation and a single respiratory cycle, respectively. Carbon ion beam distribution for each strategy was calculated as a function of respiratory phase by applying the compensating bolus to 4DCT at the respective phases. Smearing was not applied to the bolus, but consideration was given to drill diameter. The accumulated dose distributions were calculated by applying deformable registration and calculating the dose–volume histogram.
Results: Doses to normal tissues in gated treatment were minimized mainly on the inferior aspect, which thereby minimized excessive doses to normal tissues. Over 95% of the dose, however, was delivered to the clinical target volume at all phases for both treatment strategies. Maximum doses to the duodenum and pancreas averaged across all patients were 43.1/43.1 GyE (ungated/gated) and 43.2/43.2 GyE (ungated/gated), respectively.
Conclusions: Although gated treatment minimized excessive dosing to normal tissue, the difference between treatment strategies was small. Respiratory gating may not always be required in pancreatic treatment as long as dose distribution is assessed. Any application of our results to clinical use should be undertaken only after discussion with oncologists, particularly with regard to radiotherapy combined with chemotherapy. © **2010 Elsevier Inc.**

Carbon beam, Computed tomography, Four-dimensional, Pancreas, Treatment planning.

INTRODUCTION

Organ positional and geometric variations resulting from intrafractional respiratory motion degrade treatment accuracy in two ways, first by moving the tumor out of the beam field, and second by altering the radiologic pathlength (WEL = water-equivalent length) from the patient surface to the tumor (1–9). These effects degrade dose conformation in scattered and scanned charged particle beams, and also in photon beam treatments such as intensity-modulated radiotherapy and Cyberknife.

Several techniques to mitigate dose variation due to intrafractional respiratory motion have been recently introduced (10–16). Among these, respiratory-gated irradiation delivers the treatment beam at the most reproducible respiratory phase, which generally occurs around exhalation (17), and findings from several treatment centers have now been implemented (18, 19). Our previous study using four-dimensional computed tomography (4DCT) datasets in lung cases reported that WEL variation was caused by intrafractional respiratory motion (2) and that this variation could be minimized by respiratory-gated treatment (2). Although a single case was presented at the 2008 meeting of the American Society for Therapeutic Radiology and Oncology (20), we are unaware of any comprehensive comparison of respiratory-gated and respiratory-ungated treatment strategies in abdominal regions using charged particle beam.

Reprint requests to: Shinichiro Mori, Ph.D., Research Center for Charged Particle Therapy, National Institute of Radiological Sciences, Inage-ku, Chiba 263-8555, Japan. Tel: 81-43-251-2111; E-mail: shinshin@nirs.go.jp

Received Sept 18, 2008, and in revised form May 23, 2009. Accepted for publication May 26, 2009.